Cooperative distributed estimation and control of multiple autonomous vehicles for range-based underwater target localization and pursuit

Nguyen T. Hung, Francisco Rego, António M. Pascoal, *Member, IEEE*

***Abstract*— We study the problem of using single or multiple cooperative autonomous vehicles, called trackers, to localize and pursue an unknown underwater moving target using measurement of the ranges between the tracker(s) and the target. At the motion planning level, each tracker is assigned a spatial-temporal (S-T) curve to track that consists of the composition of two types of motion: along the target´s trajectory and on a path encircling the target. At the control level, we derive control laws for robust trajectory tracking and show that under mild assumptions on the convergence of the target's state estimate provided by a suitably designed filter, the tracker converges to and remains in a desired vicinity of the target.**

For the case of multiple trackers, we propose an efficient distributed estimation and control (DEC) strategy for the trackers that takes into account explicitly the constraints on the inter-tracker communication network. To this end, a distributed extended Kalman filter (DEKF) and a distributed control law for cooperative S-T curve tracking are developed to cooperatively pursue and localize the target. Using this set-up, all trackers converge to a specified vicinity of the target while keeping an optimal tracker-target relative geometry that maximizes the range information acquired to estimate the target's state. The stability of the complete closed-loop DEC system is analyzed rigorously and the efficacy of the proposed strategy is illustrated with extensive computer simulations for the 2-D and 3-D cases.

***Index Terms*— Range-based target localization, target tracking, target pursuit, distributed estimation, distributed control.**

I. INTRODUCTION

The problem of range-based simultaneous target localization and pursuit (hereafter referred to as range-based SLAP) using autonomous marine vehicles called trackers (e.g. autonomous surface or underwater vehicles) has received widespread attention in recent years due to its importance in a vast number of applications in the areas of marine science, surveillance and reconnaissance, search-and-rescue, and military operations, [1]–[5]. In this setup, the trackers are equipped with acoustic devices that measure ranges to the target and use this information to estimate the state of the latter (localization task), while keeping a desired relative geometric formation in a predefined vicinity of the target to acquire maximal range information about it for estimation purposes (pursuit task) [5], [6]. The pursuit task is extremely relevant in the marine environment since there is a limit on the maximum range that can be measured with low power acoustic equipment [7], [8]. Relevant work using unmanned aerial vehicles (UAVs) for target reconnaissance can be found in [9]. However, in this work the localization task is not necessary because the position of target is known.

In the context of range-based SLAP, the primary problem is related to the localization task. Besides the design of an appropriate target state estimator, the key issue is how to plan the motion of the trackers such that through proper maneuvering the ranges taken from the trackers to the targets provide "sufficiently rich" information for the estimation of the target's state. Technically, the answer to this problem must provide conditions on the trackers' motions such that the acquired ranges yield observability of the target motion. Using tools for observability analysis, several results on this topic were reported in [5], [10]–[18]. For instance, in [10], [18] necessary and sufficient conditions were derived on the motion of the trackers to yield observability of a target undergoing several types of motions (e.g. constant velocity or acceleration) that lead to useful guidelines for tracker motion planning. Another relevant but equivalent result was reported in [19], [20] where it is shown that in order for the target to be observable the velocity of the tracker must be persistently exciting. On a different and yet complementary vein, the Fisher Information Matrix (FIM) has been used to study the observability of a given system from a quantitative standpoint, borrowing tools from estimation theory. See for example [5], [17] for applications of this methodology to target tracking that involve the computation of the range-based information available as a function of relative tracker-target motion and how it impacts on the their optimal relative geometric configurations. See also [21] for an interesting application of the FIM to the computation of optimal trajectories for a group of unmanned aerial vehicles (UAVs) to track a given target.

The second problem relates to the pursuit task, that is, how to

This research was supported by the following projects: H2020 EU Marine Robotics Research Infrastructure Network (GA 731103), H2020-EU.1.2.2 - FET Proactive RAMONES (GA 101017808), POCI-01-0247-FEDER-024508-OCEANTECH / Portugal 2020 through Compete 2020, and LARSyS-FCT No. UIDB/50009/2020. The first author received funding from the +Atlantic Collaborative Lab.

Nguyen T. Hung and António M. Pascoal are with ISR/IST, University of Lisbon, Lisbon, Portugal (nguyen.hung@tecnico.ulisboa.pt, antonio@isr.tecnico.ulisboa.pt). Francisco Rego is with ISR/IST, Lisbon, Portugal and the CoLAB +Atlantic, Portugal. (francisco.rego@colabatlantic.com).

control the vehicles such that they converge to a vicinity of the target while holding a desired relative geometric formation with access to range measurements only. Several solutions to this problem are presented in the literature [5], [22], [23]. For example, a possible solution is to estimate the position of the target and then use this information to design a tracking controller to pursue the target [5], [23]. With this approach, the localization and pursuit tasks are tightly coupled. A solution that does not require an explicit estimation step is reported in [22]. However, this approach requires that the time derivative of the range measurement be available to the tracker.

From a theoretical standpoint, the range-based SLAP problem can be solved with only one tracker or a set of multiple trackers, see some preliminary results on observability analysis in [5], [17], [18]. Each scenario has its own advantages and disadvantages and technical challenges. It is obvious that using only one tracker is more cost-effective and easier to implement. However, using multiple trackers potentially enhances both the performance and robustness of the localization and pursuit system. In addition, as shown in [17], [18], using multiple trackers makes the motions of the latter smoother. The intrinsic problem when using multiple trackers is how to make them cooperate in an efficient manner in order to localize and pursue a target. To address this problem, a receding horizon planing, control and estimation framework was proposed in [5] to solve the problem in a centralized manner. However, it might be difficult and inefficient to implement this approach in practice when the trackers are distributed over a large spatial region. A more efficient approach in terms of data exchanged among the trackers consists of using a distributed state estimation framework, where each tracker estimates independently the state of the target using its own measurements and reduced additional information received from the neighboring trackers. Due to the growing interest in wireless sensor networks, the problem of distributed state estimation has received great attention in recent years. This led to the development of many methods to tackle the nonlinear distributed estimation problem based on classical techniques such as extended Kalman filtering [24] (consensus-type method), moving horizon estimation [25], and particle filtering [26]. For a survey of solutions to this problem the reader is refereed to [27].

Motivated by the above considerations, we propose a systematic approach to solve the problem of range-based SLAP for 2-D and 3-D cases with *i) a single autonomous vehicle and ii) multiple autonomous vehicles.* Specifically, the main contributions include the following:

(i) Inspired by recent results on observability analysis in [18] and optimal tracker motion planing in [5] in the context of range-based target localization, a trajectory in the form of S-T curve is computed for each tracker to go through. By parameterizing the curves appropriately it can be guaranteed that if the trackers track the desired S-T curves accurately, then the target motions become observable and, at the same time, the trackers converge to an optimal desired relative formation that, in a well defined mathematical sense, renders the range-information acquired "maximal" for target state estimation purposes.

(ii) Two types of trajectory tracking controllers that use the estimated target's state are derived for the trackers to track the desired S-T curves. The controllers are shown to be robust against bounded errors in the estimate of the target's state.

(iii) For the case of multiple trackers, we propose an efficient distributed estimation and control (DEC) strategy for the trackers to localize and pursue the target in a cooperative manner. The proposed DEC ensures that asymptotically, all trackers reach consensus on the estimates of the target's state and maintain a desired geometrical formation in a vicinity of the target. The proposed strategy requires very limited information to be exchanged among the trackers, thus making it very efficient for practical implementation.

The paper is organized as follows. Section II summarizes the basic notation and background on algebraic graph theory that is essential to the design of distributed estimation and control systems. The simultaneous target localization and pursuit problem is formulated in Section III. Its solution using single and multiple trackers is described in Sections IV and V, respectively. Illustrative simulations are presented in Section VI. Section VII contains the main conclusions and a brief discussion of issues that warrant further research effort.

II. NOTATION AND ALGEBRAIC GRAPH THEORY

A. Notation

In what follows, we let $\mathbb{R}, \mathbb{R}_{>0}$, and $\mathbb{R}_{\geq 0}$ denote the set of real, positive real, and nonnegative real numbers, respectively. We shall use the notation $\|\cdot\|$ to denote the Euclidean norm of a vector in $\mathbb{R}^n$. Given matrices $A, B \in \mathbb{R}^{n\times n}$ the notation $A \succeq B$ means that $A - B$ is positive semi-definite. A continuous function $\alpha : [0, a) \to [0, \infty)$ is said to be of class $\mathcal{K}$ if it is strictly increasing and $\alpha(0) = 0$ and of class $\mathcal{K}_\infty$ if $a = \infty, \alpha(0) = 0$, and $\alpha(r) \to \infty$ as $r \to \infty$. A continuous function $\beta : [0, a) \times [0, \infty) \to [0, \infty)$ is said to be of class $\mathcal{KL}$ if, for each fixed s, the mapping $\beta(r, s)$ is of class $\mathcal{K}$ with respect to r and, for each fixed r, the mapping $\beta(r, s)$ is decreasing with respect to s and $\beta(r, s) \to 0$ as $s \to \infty$. Given a symmetric matrix A, the symbols $\lambda_{\min}(A)$ and $\lambda_{\max}(A)$ denote the smallest and the largest eigenvalues of A. Given vectors $\mathbf{x}_i \in \mathbb{R}^n; i = 1, ..., N$, $\text{col}(\mathbf{x}_1, ..., \mathbf{x}_N) \triangleq [\mathbf{x}_1^\top, ..., \mathbf{x}_N^\top]^\top \in \mathbb{R}^{n\times N}$. The notation $\mathcal{N}(\boldsymbol{\mu}, P)$ denotes a Gaussian (normal) distribution with mean $\boldsymbol{\mu}$ and covariance matrix P.

B. Algebraic graph theory

Consider a digraph $\mathcal{G} = \mathcal{G}(\mathcal{V}, \mathcal{E}, \mathcal{A})$ induced by the communication network of a multi-agent system that consists of a set of N vertices (nodes) $\mathcal{V} = \{1, 2, ...N\}$, a set of directed edges $\mathcal{E} \subseteq \mathcal{V} \times \mathcal{V}$, and an adjacency matrix $\mathcal{A} = [a_{ij}] \in \mathbb{R}^{N\times N}$. The later satisfies the conditions $a_{ij} = 1$ if $(j, i) \in \mathcal{E}$ and $a_{ij} = 0$ otherwise. Here, self-edges (i, i) are not allowed and hence $a_{ii} = 0$. A path from vertex i to vertex j is an ordered sequence of vertices such that each immediate pair of the vertices is an edge. A digraph is strongly connected if

there exists a path from any $i \in \mathcal{V}$ to any $j \in \mathcal{V}$. The set of in-neighbors and the set of out-neighbors of vertex i are defined as $\mathcal{N}_{\text{in}}^{[i]} = \{j \in \mathcal{V} : (j,i) \in \mathcal{E}\}$ and $\mathcal{N}_{\text{out}}^{[i]} = \{j \in \mathcal{V} : (i,j) \in \mathcal{E}\}$, respectively. The in- and out- degree matrices D_{in} and D_{out} are defined as $D_{\text{in}} = \text{diag}(d_{\text{in}}^{[i]})$ and $D_{\text{out}} = \text{diag}(d_{\text{out}}^{[i]})$ where

$$d_{\text{in}}^{[i]} = \sum_{j \in \mathcal{N}_{\text{in}}^{[i]}} a_{ij} \qquad \text{and} \qquad d_{\text{out}}^{[i]} = \sum_{j \in \mathcal{N}_{\text{out}}^{[i]}} a_{ji}.$$

The Laplacian matrix L of a digraph $\mathcal{G}$ is defined by $L = D_{\text{in}} - \mathcal{A}$. If $\mathcal{G}$ is strongly connected, then 0 is a simple eigenvalue of L with associated eigenvector $\mathbf{1} := [1]_{N\times 1} \in \mathbb{R}^N$.

Remark 1: With the graphs defined as above, we use the convention that an agent i can receive information from neighbors in $\mathcal{N}_{\text{in}}^{[i]}$ and send information to neighbors in $\mathcal{N}_{\text{out}}^{[i]}$. The following lemmas will be used in this paper.

Lemma 1 ([[28], [29]): Suppose that the graph $\mathcal{G}$ is strongly connected. Then, there is a positive left eigenvector $\mathbf{r} = [r_1, ..., r_N]^\top \in \mathbb{R}^N$ of L associated with the zero eigenvalue that satisfies $\mathbf{r}^\top \mathbf{1} = 1$ and $RL + L^\top R \succeq 0$, where $R = \text{diag}(r_1, ..., r_N) \in \mathbb{R}^{N\times N}$.

Definition 1 (Generalized algebraic connectivity, [28]): Let L be the Laplacian matrix of a strongly connected digraph $\mathcal{G}$. The generalized algebraic connectivity of the graph is defined as

$$a(L) = \min_{\mathbf{x}\neq \mathbf{0} \text{ and } \mathbf{x}\perp \mathbf{r}} \frac{\mathbf{x}^\top (RL + L^\top R)\mathbf{x}}{2\mathbf{x}^\top R\mathbf{x}}, \tag{1}$$

where R is defined in Lemma 1. For undirected graphs, $a(L) = \lambda_2(L)$, where the latter is called the Fiedler eigenvalue of the graph.

III. PROBLEM FORMULATION AND BACKGROUND RESULTS

A. Problem formulation

1) Tracker' model: Consider a group of $N(N \geq 1)$ autonomous vehicles, henceforth called trackers, charged with the task of localizing and pursuing a moving target. In what follows, $\{\mathcal{I}\} = \{x_\mathcal{I}, y_\mathcal{I}, z_\mathcal{I}\}$ denotes a inertial frame and $\{\mathcal{B}\}^{[i]} = \{x_\mathcal{B}^{[i]}, y_\mathcal{B}^{[i]}, z_\mathcal{B}^{[i]}\}$ denotes a body frame attached to tracker i; $i \in \mathcal{V}$. For each $i \in \mathcal{V}$, let $\mathbf{p}^{[i]} \in \mathbb{R}^3$ be the inertial position vector of the tracker expressed in $\{\mathcal{I}\}$, and $\mathbf{v}^{[i]} = [v_1^{[i]}, v_2^{[i]}, v_3^{[i]}]^\text{T}$ its velocity vector expressed in the body frame $\{\mathcal{B}\}^{[i]}$, consisting of surge $(v_1^{[i]})$, sway $(v_2^{[i]})$, and heave $(v_3^{[i]})$ speed components. The tracker' kinematic model is given by

$$\dot{\mathbf{p}}^{[i]} = R(\boldsymbol{\eta}^{[i]})\mathbf{v}^{[i]}, \tag{2}$$

where $R(\boldsymbol{\eta}^{[i]}) \in SO(3)$[1] is the rotation matrix from $\{\mathcal{B}\}^{[i]}$ to $\{\mathcal{I}\}$, locally parameterized by a vector $\boldsymbol{\eta}^{[i]} \triangleq [\phi^{[i]}, \theta^{[i]}, \psi^{[i]}]^\text{T}$ that contains the Euler angles of roll $(\phi^{[i]})$, pitch $(\theta^{[i]})$ and yaw $(\psi^{[i]})$. Note that the time derivative of the rotation matrix satisfies

$$\dot{R}(\boldsymbol{\eta}^{[i]}) = R(\boldsymbol{\eta}^{[i]})S(\boldsymbol{\omega}^{[i]}), \tag{3}$$

[1] $SO(3) \triangleq \{R \in \mathbb{R}^{3\times 3} : RR^\text{T} = I_3, \det(R) = 1\}$

where $\boldsymbol{\omega}^{[i]} = [p^{[i]}, q^{[i]}, r^{[i]}]^\text{T}$ is the body-fixed angular velocity vector and S is a skew-symmetric matrix defined as

$$S(\boldsymbol{\omega}^{[i]}) = \begin{bmatrix} 0 & -r^{[i]} & p^{[i]} \\ r^{[i]} & 0 & -q^{[i]} \\ -p^{[i]} & q^{[i]} & 0 \end{bmatrix}. \tag{4}$$

In the present paper, for simplicity of presentation, we consider that the trackers are under-actuated vehicles for which the sway and heave speeds are negligible, i.e. $\mathbf{v}^{[i]} = [v_1^{[i]}, 0, 0]; i \in \mathcal{V}$. The input of each tracker i is therefore defined as

$$\mathbf{u}^{[i]} = [v_1^{[i]}, p^{[i]}, q^{[i]}, r^{[i]}]^\text{T} \in \mathbb{R}^4, \tag{5}$$

consisting of surge speed $v_1^{[i]}$ and angular velocity $\boldsymbol{\omega}^{[i]}$.

Remark 2: For the **2-D** *case, e.g. when the trackers are restricted to move in the $x_\mathcal{I} - y_\mathcal{I}$ horizontal plane, the tracker's model* (2) *applies with $\boldsymbol{\eta}^{[i]} = \psi^{[i]}$ and $\boldsymbol{\omega}^{[i]} = r^{[i]}$. In this case, the tracker's control inputs include the surge speed and the yaw rate, i.e. $\mathbf{u}^{[i]} = [v_1^{[i]}, r^{[i]}]^\text{T} \in \mathbb{R}^2$ and $S(\boldsymbol{\omega}^{[i]}) = \begin{bmatrix} 0 & -r^{[i]} \\ r^{[i]} & 0 \end{bmatrix}$. In practice, the tracker's model* (2) *is adequate for a wide class of under-actuated marine vehicles of which Medusa and Delfim ([30]) and Charlie ([31]) are representative examples.*

2) Target's model: Let $\mathbf{q}(t) \in \mathbb{R}^3$ be the target's trajectory to be tracked, and $\boldsymbol{v}(t) = \dot{\mathbf{q}}(t)$ be the target velocity vector, both expressed in $\{\mathcal{I}\}$. Even though the target's trajectory is unknown, we assume that the target changes its velocity slowly that its motion can be described by a quasi-steady model of the form

$$\dot{\mathbf{x}}(t) = A\mathbf{x}(t) + \mathbf{w}(t), \tag{6}$$

where $\mathbf{x}(t) = [\mathbf{q}^\text{T}(t), \boldsymbol{v}^\text{T}(t)]^\text{T} \in \mathbb{R}^6$ is the state of the target, $\boldsymbol{v}(t)$ is slowly varying, $\mathbf{w} \sim \mathcal{N}(\mathbf{0}, Q_t)$ is a zero mean Gaussian process noise with covariance Q_t and $A = \begin{bmatrix} 0 & I_3 \\ 0 & 0 \end{bmatrix}$. Let $\mathbf{x}_k = [\mathbf{q}_k^\text{T}, \boldsymbol{v}_k^\text{T}]^\text{T} \in \mathbb{R}^6$ be the state of the target, at the discrete time $k; k \in \mathbb{N}$. For target state estimation purposes (e.g. using a discrete EKF), (6) can be discretized using Euler's method, yielding

$$\mathbf{x}_{k+1} = F\mathbf{x}_k + \mathbf{w}_k, \tag{7}$$

where

$$F = \begin{bmatrix} I_3 & T_s I_3 \\ 0_{3\times 3} & I_3 \end{bmatrix}, \tag{8}$$

T_s is the sampling period, and $\mathbf{w}_k \sim \mathcal{N}(\mathbf{0}, Q); Q = T_s^2 Q_t$.

Remark 3: For the 2-D case, the target model (7) *applies with $\mathbf{x} \in \mathbb{R}^4$ and $F = \begin{bmatrix} I_2 & T_s I_2 \\ 0_{2\times 2} & I_2 \end{bmatrix}$.*

3) Range measurement model: Assume that each tracker i is equipped with an acoustic unit that measures its distance to the target. Let also $d_k^{[i]}$ be the true distance between tracker $i; i \in \mathcal{V}$ and the target at discrete time k, defined as

$$d_k^{[i]} = \left\| \mathbf{p}_k^{[i]} - \mathbf{q}_k \right\|, \tag{9}$$

where $\mathbf{p}_k^{[i]}$ denotes the position of tracker i at discrete time instant k. Further, let $y_k^{[i]}$ denote the range measurements

which, we assume, are corrupted by white Gaussian noise according to the range measurement model

$$y_k^{[i]} = d_k^{[i]} + \eta_k^{[i]}, \tag{10}$$

where $\eta_k^{[i]} \sim \mathcal{N}(0, \sigma); i \in \mathcal{V}$ is Gaussian measurement noise. The cooperative target localization and pursuit problem that is the main topic of this paper can now be formally defined as follows.

Problem 1 (Cooperative target localization and pursuit): Consider a group of $N(N \geq 1)$ trackers, with models described by (2) *that are in charge of localizing and pursuing an unknown target whose dynamics are described by* (6)*. Assume the trackers' inter-communication network is modeled by a digraph $\mathcal{G}$. Suppose that the trackers' positions and orientations are known. Assume further that the trackers can measure ranges to the target according to the measurement equation* (10)*. Let $\hat{\mathbf{x}}^{[i]}$ denote an estimate of the target's state $\mathbf{x}$ computed by tracker i. Design a distributed control law for $\mathbf{u}^{[i]}; i \in \mathcal{V}$ and a distributed estimation algorithm for $\hat{\mathbf{x}}^{[i]}; i \in \mathcal{V}$ to fulfill the following tasks:*

- *Cooperative pursuit: ensure that asymptotically all trackers stay in a given vicinity of the target, i.e.*

$$\lim_{t\to\infty} \left\| \mathbf{p}^{[i]}(t) - \mathbf{q}(t) \right\| \leq r_c, \tag{11}$$

  for a given r_c.
- *Cooperative localization (estimation): ensure that all estimates $\hat{\mathbf{x}}^{[i]}$ of the target's sate reach consensus, that is,*

$$\lim_{k\to\infty} \left\| \hat{\mathbf{x}}_k^{[i]} - \mathbf{x}_k \right\| \leq r_e \tag{12}$$

for all $i = 1, ...N$, where r_c, and r_e are given positive values.

Remark 4: The problem formulation above can be easily extended to the cases where the trackers and the target move in different horizontal planes, e.g. when the trackers are at the surface while the target is underwater with a known depth. In this scenario, (11) *implies that the trackers should remain in a desired 2-D region centered at the projection of the target on the surface horizontal plane.*

B. Background results

In this subsection, we briefly recall some preliminary results on target motion observability and optimal tracker trajectory generation for range-based target localization. The results described will be used to plan the motion for the trackers in the next section.

1) Result 1: single tracker-single target: Consider the scenario where one tracker is used to localize a target moving with unknown constant velocity i.e. $\boldsymbol{v}(t)$ is constant. As shown in [18], in a 2-D setting the target's state (position and velocity) is observable, i.e. the target's state is uniquely determined if the trajectory of the tracker belongs to a class of "cycloid-type" trajectories defined by $\mathbf{p}(t) = [p_x(t), p_y(t)]^\top = [r_x \sin(\omega t) + c_x t, r_y \cos(\omega t) + c_y t]^\top$ with $r_x, r_y, \omega \neq 0$. Furthermore, using the Fisher Information Matrix (FIM) as a means to quantifying the range information available for target estimation, it was shown that a class of optimal trajectories that maximize range information consists of having the tracker encircle the target, see [5], [17]. In 3-D, any "helix-type" trajectory defined by $\mathbf{p}(t) = [r_x \sin(\omega_1 t) + c_x t, r_y \cos(\omega_1 t) + c_y t, r_z \sin(\omega_2 t) + c_z t]^\top$ with $r_x, r_y, r_z, \omega_1 \neq \omega_2 \neq 0$ guarantees observability of the target's state, see Theorem 2 in [18].

2) Result 2: two trackers-single target: Consider the scenario where two trackers are used to localize a target. In this case, the target's state is completely observable at an arbitrarily time t_0 if and only if the columns of matrix $\mathcal{O}(t)$, defined by

$$\mathcal{O}(t) \triangleq [(\mathbf{p}^{[2]}(t) - \mathbf{p}^{[1]}(t))^\top \quad (t - t_0)(\mathbf{p}^{[2]}(t) - \mathbf{p}^{[1]}(t))^\top], \tag{13}$$

are linearly independent on an interval $[t_0, t]$ for some $t > t_0$, see Theorem 5 in [18]. In the 2-D case, it was shown in [5] that the optimal trajectories for the tracker that maximize the range-information available for estimating the target's state are the ones satisfying

$$(\mathbf{p}_k^{[1]} - \mathbf{q}_k) \perp (\mathbf{p}_k^{[2]} - \mathbf{q}_k) \tag{14}$$

for all range measurement time instants k, i.e. the relative position vectors from each tracker to the target are orthogonal, see Proposition 2 in [5]. Note that this tracker-target geometry is optimal for target state estimation for the cases where the target's velocity vector is known, see [5], [17].

3) Result 3: N trackers-single target: If N trackers $(N \geq 3)$ are used to localize the target, it was shown in in [5], Proposition 3, for the 2-D case that the optimal tracker trajectories for target state estimation are the ones for which the trackers' positions are distributed uniformly around the target and the angle made by the relative vectors from two adjacent trackers to the target is $2\pi/N$. This result is illustrated in Fig. III.1 for the case of three trackers.

In the next section, we will use the aforementioned knowledge to plan optimal trajectories for the trackers and design a cooperative distributed control and estimation strategy to simultaneously localize and pursue the target.

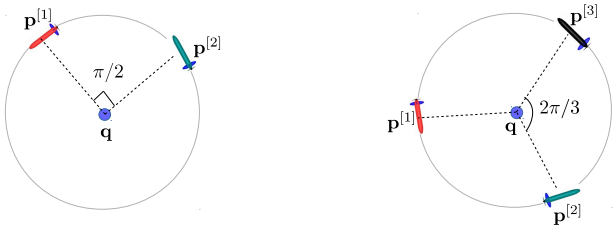

Fig. III.1: Examples of optimal relative tracker-target geometries that maximize the information available to estimate the target's state. (Left: $N = 2$, Right: $N = 3$). Positions: $\mathbf{q}$ (target), $\mathbf{p}^{[i]}$ (trackers).

IV. TARGET LOCALIZATION AND PURSUIT WITH ONE TRACKER

We start by consider a scenario where only one tracker is used to localize and pursue a target. In this case, for the sake of clarity we drop the superscript $[i]$ in the relevant variables in this section. In what follows we derive a desired trajectory for the tracker, together with the corresponding trajectory tracking controllers.

A. A trajectory tracking strategy for target pursuit

For the purpose of illustrating the underlying idea of the proposed method, we assume that the target's position $\mathbf{q}(t)$ and its velocity $\boldsymbol{v}(t)$ are known. This assumption will be relaxed in the next subsection. Let $\mathcal{P} : \gamma \to \mathbf{r}(\gamma) \in \mathbb{R}^3$ be a path defined in an inertial frame, given by

$$\mathbf{r}(\gamma) = [r_{\mathrm{x}} \cos(\gamma+\gamma_0), r_{\mathrm{y}} \sin(\gamma+\gamma_0), r_{\mathrm{z}} \sin(\frac{\gamma}{c}+\gamma_0)]^\top, \quad (15)$$

where γ is a path parameterizing variable (e.g. path length), and $r_{\mathrm{x}}, r_{\mathrm{y}}, r_{\mathrm{z}} \in \mathbb{R}_+, c \in \mathbb{R} \setminus \{0, 1\}$ and $\gamma_0 \in \mathbb{R}$ are constant parameters. For the 2D-case, $\mathbf{r}(\gamma) \in \mathbb{R}^2$ is defined as

$$\mathbf{r}(\gamma) = [r_{\mathrm{x}} \cos(\gamma + \gamma_0), r_{\mathrm{y}} \sin(\gamma + \gamma_0)]^\top. \quad (16)$$

Borrowing the concept of moving path following (MPF) proposed in [32], [33] we let $\mathbf{p}_{\mathrm{d}} : \mathbb{R} \times \mathbb{R}_{\geq 0} \to \mathbb{R}^3$ be a desired S-T curve that consists of the composition of motions along the target and along a path around the target, defined as

$$\mathbf{p}_{\mathrm{d}}(t) = \mathbf{r}(\gamma(t)) + \mathbf{q}(t), \quad (17)$$

where the spatial part $\mathbf{r}(\gamma)$ is described by (15) and (16)

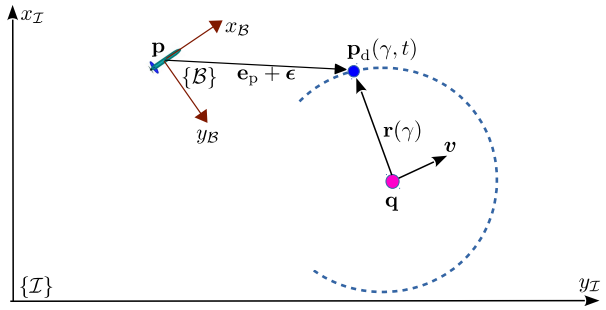

Fig. IV.1: Illustration of the proposed methodology in 2-D.

for the 3-D and 2-D cases, respectively. The underlying idea behind the method proposed for target pursuit is that if the tracker can be controlled s.t. $\mathbf{p} \to \mathbf{p}_{\mathrm{d}}$, then it will converge to a vicinity of the target defined by $\mathbf{r}$, i.e. $\|\mathbf{p} - \mathbf{q}\| \to \|\mathbf{r}(\gamma)\| \overset{(15)}{\leq} \sqrt{r_{\mathrm{x}}^2 + r_{\mathrm{y}}^2 + r_{\mathrm{z}}^2}$ for all γ. For reasons that will become clear latter, γ is allowed to be a function of time, with dynamics to be chosen appropriately to shape the approach of the tracker to the desired S-T curve. Furthermore, if the dynamics of γ can be chosen s.t. $\dot{\gamma} \to \omega_{\mathrm{d}}$, where

$$\omega_{\mathrm{d}} = \bar{\omega}, \quad (18)$$

with a constant $\bar{\omega} \neq 0$, then the tracker will encircle the target with angular rate $\bar{\omega}$. For the 2-D case, the S-T curve described by (17) that the tracker must track takes the form of the optimal trajectories for range-based target localization, while for 3-D case, it ensures the observability of the target's state, see Section III-B.1.

Inspired from the work in [34] we now derive two tracking controllers for the tracker in order have it pursue and encircle the target. To this end, define

$$\begin{aligned} \mathbf{e}_{\mathrm{p}} &= R^\top(\boldsymbol{\eta})(\mathbf{p} - \mathbf{p}_{\mathrm{d}}) - \boldsymbol{\epsilon} \\ &\overset{(17)}{=} R^\top(\boldsymbol{\eta})(\mathbf{p} - \mathbf{r}(\gamma) - \mathbf{q}) - \boldsymbol{\epsilon} \end{aligned} \quad (19)$$

as the position error between the tracker and the desired trajectory expressed in the tracker's body frame $\{\mathcal{B}\}$, where $\boldsymbol{\epsilon}$ is an arbitrarily small non-zero vector, see the illustration of this error for the case of 2D in Fig.IV.1. The idea behind the use of vector $\boldsymbol{\epsilon}$ was originally introduced in [34] and will become clear next. By definition, if $\mathbf{e}_{\mathrm{p}}$ converges to zero then the tracker converges to the vicinity of the target centered at the target with radius $\|\mathbf{r}\| + \|\boldsymbol{\epsilon}\|$. Clearly, by proper choice of $r_{\mathrm{x}}, r_{\mathrm{y}}, r_{\mathrm{z}}$, and $\boldsymbol{\epsilon}$ s.t. $\|\mathbf{r}(\gamma)\| + \|\boldsymbol{\epsilon}\| \leq r_c$ for all γ the pursuit task described by (11) will be fulfilled. Define also

$$e_\gamma = \dot{\gamma} - \omega_{\mathrm{d}} \quad (20)$$

as the speed tracking error for the temporal evolution of γ. Let $\mathbf{e} = [\mathbf{e}_{\mathrm{p}}^\top, e_\gamma]^\top$ be the complete tracking error vector. Our main objective is to derive tracking control laws for $\mathbf{u}$ defined in (5) to drive $\mathbf{e}$ to zero. Taking the time derivative of (19) and using (2),(3),(4), (5) yields the dynamics of $\mathbf{e}_{\mathrm{p}}$, given as

$$\begin{aligned} \dot{\mathbf{e}}_{\mathrm{p}} &= -S(\boldsymbol{\omega})\mathbf{e}_{\mathrm{p}} - S(\boldsymbol{\omega})\boldsymbol{\epsilon} + \mathbf{v} - R^\top(\boldsymbol{\eta})\left(\mathbf{r}'(\gamma)\dot{\gamma} + \boldsymbol{v}\right) \\ &= -S(\boldsymbol{\omega})\mathbf{e}_{\mathrm{p}} + \Delta\mathbf{u} - R^\top(\boldsymbol{\eta})\left(\mathbf{r}'(\gamma)\dot{\gamma} + \boldsymbol{v}\right) \end{aligned} \quad (21)$$

where $\mathbf{r}'(\gamma) \triangleq \frac{\partial \mathbf{r}(\gamma)}{\partial \gamma}$, and

$$\Delta = \begin{bmatrix} 1 & 0 & -\epsilon_3 & \epsilon_2 \\ 0 & \epsilon_3 & 0 & -\epsilon_1 \\ 0 & -\epsilon_2 & \epsilon_1 & 0 \end{bmatrix}, \Delta = \begin{bmatrix} 1 & \epsilon_2 \\ 0 & -\epsilon_1 \end{bmatrix} \quad (22)$$

for the 3-D and the 2-D case, respectively where ϵ_i denotes the i^{th} component of vector $\boldsymbol{\epsilon}$. From (20) the dynamics of the error e_γ are described by

$$\dot{e}_\gamma = \ddot{\gamma}. \quad (23)$$

To drive the tracking error $\mathbf{e}$ to zero, the following controllers can be used:

Tracking Controller - Type I

$$\begin{aligned} \mathbf{u} &= \boldsymbol{k}(\mathbf{x}) \\ \dot{\gamma} &= \omega_{\mathrm{d}}. \end{aligned} \quad (24)$$

Tracking Controller - Type II

$$\begin{aligned} \mathbf{u} &= \boldsymbol{k}(\mathbf{x}) \\ \ddot{\gamma} &= -k_\gamma e_\gamma + \mathbf{e}_{\mathrm{p}}^\top R^\top(\boldsymbol{\eta})\mathbf{r}'(\gamma), \end{aligned} \quad (25)$$

with $\boldsymbol{k}(\mathbf{x})$ given by

$$\boldsymbol{k}(\mathbf{x}) = \bar{\Delta}\left(R^\top(\boldsymbol{\eta})\left(\mathbf{r}'(\gamma)\omega_{\mathrm{d}} + \boldsymbol{v}\right) - K_{\mathrm{p}}\mathbf{e}_{\mathrm{p}}\right), \quad (26)$$

where $\bar{\Delta} = \Delta^\top(\Delta\Delta^\top)^{-1}$, K_{p} is a positive definite matrix with appropriate dimension, $k_\gamma > 0$, and ω_{d} is given by (18). With the proposed controllers, we obtain the following result.

Lemma 2: Consider the tracking error system described by (21) *and* (23). *Suppose that the target's state* $\mathbf{x}$ *(including both the position* $\mathbf{q}$ *and velocity* $\boldsymbol{v}$*) is completely known. Then, both tracking controllers given by* (24) *and* (25) *guarantee that the tracking error* $\mathbf{e}$ *converges to zero exponentially fast.*

Proof: See Appendix.

Remark 5: The main difference between Controller-Type I given by (24) *and Controller-Type II given by* (25) *is the strategy to control the evolution of the path parameter* γ. *With the first the derivative of* γ *is fixed, whereas with the second the dynamics of* γ *depends on feedback terms from the tracking*

error. The first is clearly simpler to implement, yet thanks to the feedback, the second has the potential to speed up the convergence of the tracking error to zero.

Remark 6: In (19)*, imposing* $\boldsymbol{\epsilon}$ *as a non-zero vector is made to ensure that the matrix* $\bar{\Delta}$ *non-singular, thus ensuring that the proposed controllers given by* (24) *and* (25) *are well-defined.*

B. Unknown target pursuit

In the previous section, we showed that if the target's state is fully known, then both control laws (24) and (25) steer the tracker to a vicinity of the target and encircle it with a desired angular speed $\omega_{\rm d} = \bar{\omega}$. The convergence rate was shown to be exponential. However, in the context of range-based SLAP, the target's state is unknown, and must be estimated on-line. To address this problem, we suppose that the tracker is equipped with a filter, which is capable of estimating the target's state (both the target's position and velocity vectors). This can be done using the target model given in (8) and the range measurement model (10), as explained later. Let $\hat{\mathbf{x}} = [\hat{\mathbf{q}}, \hat{\boldsymbol{v}}]$ be the estimate of the target's state $\mathbf{x}$, where $\hat{\mathbf{q}}$ denotes an estimate of the true target position vector $\mathbf{q}$, while $\hat{\boldsymbol{v}}$ denotes the estimate of the true target velocity vector $\boldsymbol{v}$. Define also

$$\hat{\mathbf{e}}_{\rm p} = R^{\top}(\boldsymbol{\eta})\left(\mathbf{p} - \mathbf{r}(\gamma) - \hat{\mathbf{q}}\right) - \boldsymbol{\epsilon} \tag{27}$$

which is similar to (19) but the estimated target position $(\hat{\mathbf{q}})$ is used, instead of the true target position $\mathbf{q}$. The following control laws are proposed for unknown target pursuit.

Tracking Controller - Type I - Unknown Target

$$\begin{aligned} \mathbf{u} &= \boldsymbol{k}(\hat{\mathbf{x}}) \\ \dot{\gamma} &= \omega_{\rm d}. \end{aligned} \tag{28}$$

Tracking Controller - Type II - Unknown Target

$$\begin{aligned} \mathbf{u} &= \boldsymbol{k}(\hat{\mathbf{x}}) \\ \ddot{\gamma} &= -k_{\gamma} e_{\gamma} + \hat{\mathbf{e}}_{\rm p}^{\top} R^{\top}(\boldsymbol{\eta}) \mathbf{r}'(\gamma), \end{aligned} \tag{29}$$

where e_{γ} is given by (20), $\omega_{\rm d}$ is given by (18), and

$$\boldsymbol{k}(\hat{\mathbf{x}}) = \bar{\Delta}\left(R^{\top}(\boldsymbol{\eta})\left(\mathbf{r}'(\gamma)\omega_{\rm d} + \hat{\boldsymbol{v}}\right) - K_{\rm p}\hat{\mathbf{e}}_{\rm p}\right). \tag{30}$$

where $\hat{\mathbf{e}}_{\rm p}$ is given by (27). Let $\tilde{\mathbf{x}}$ be the estimation error of the target's state, defined as

$$\tilde{\mathbf{x}} = \hat{\mathbf{x}} - \mathbf{x}. \tag{31}$$

The following theorem states the main result on single tracker target pursuit.

Theorem 1: Consider the tracking error system described by (21) *and* (23)*. Then, the controllers given by* (28) *and* (29) *guarantee that the tracking error system is input-to state stable (ISS) with respect to the state* $\mathbf{e}$ *and the input* $\tilde{\mathbf{x}}$*, i.e. there exist* $\beta \in \mathcal{KL}$ *and* $\alpha \in \mathcal{K}$ *functions that satisfy*

$$\|\mathbf{e}\| \leq \beta(\|\mathbf{e}(0)\|, t) + \alpha(\sup_{t \geq 0} \|\tilde{\mathbf{x}}(t)\|) \tag{32}$$

for any initial condition $\mathbf{e}(0)$.

Proof: See the Appendix.

The theorem implies that the tracking controllers (28) and (29) are robust against the estimation error $\tilde{\mathbf{x}}$, i.e. the tracking error $\mathbf{e}$ is bounded for any bounded estimation error $\tilde{\mathbf{x}}$. In addition, inequality (32) implies that asymptotically, the tracking error $\mathbf{e}$ depends only on the estimation error $\tilde{\mathbf{x}}$ and, if $\tilde{\mathbf{x}}$ converges to zero, then $\mathbf{e}$ converges to zero as well. Clearly, the above analyses imply that the tracking error depends only on the performance of the filter that estimates the target's state.

In the context of the present paper, for the sake of simplicity we adopt an EKF in information form (also called the information filter in the literature) to estimate the target's state. Note that the information form and the standard form of EKF are equivalent. The latter propagates the covariance matrix of the estimated state, whereas the former propagates the inverse of the covariance matrix. We use the information form because it is more convenient to decentralize the filter in the case of multiple trackers, to be studied later, where a distributed EKF is required to address the constraint on the inter-tracker communication network [35].

The EKF in information form is described as follows. Let $Y_k \triangleq \{y_m\}_{m=0}^{k}$ denote the set of ranges from the tracker to the target acquired up to time k. Let also $p(\mathbf{x}_k|Y_{k-1}) \sim \mathcal{N}(\hat{\mathbf{x}}_{k|k-1}, P_{k|k-1})$ and $p(\mathbf{x}_k|Y_k) \sim \mathcal{N}(\hat{\mathbf{x}}_{k|k}, P_{k|k})$ be the prior and posterior densities of the target's state, estimated at time k, respectively. Denote by $\mathbf{z}$ and Ω the information vector and the information matrix, respectively, defined as

$$\begin{aligned} \mathbf{z}_{k|k-1} &\triangleq P_{k|k-1}^{-1}\hat{\mathbf{x}}_{k|k-1} & \mathbf{z}_{k|k} &\triangleq P_{k|k}^{-1}\hat{\mathbf{x}}_{k|k} \\ \Omega_{k|k-1} &\triangleq P_{k|k-1}^{-1} & \Omega_{k|k} &\triangleq P_{k|k}^{-1}. \end{aligned} \tag{33}$$

With the above definition, the prior and posterior densities of the target can be computed recursively using Algorithm 1 below. In the algorithm, V is an arbitrarily positive definite matrix of appropriate dimensions [24]. However, V is normally chosen as the covariance matrix of the measurement noise. With the range measurement model (10), $V = \sigma$. With the EKF, the estimation error $\tilde{\mathbf{x}}$ is guaranteed to be bounded provided that the estimate of the target's state is initialized sufficiently close to the true target's state, and the process and measurement noises are sufficiently small [36].

V. TARGET LOCALIZATION AND PURSUIT WITH MULTIPLE TRACKERS

In this section, we consider scenarios where multiple trackers are used in a cooperative manner to localize and pursue the target. The use of multiple trackers potentially enhances both performance and robustness of the target localization and pursuit system. Intuitively, more trackers means that more range measurements can be acquired on a given interval and, therefore, more information is available to estimate the target's state. Multiple trackers also implies that redundant trackers are always available in cases any trackers in the group fail their mission or must leave it for any reason. However, both from a theoretical and practical standpoint, the use of multiple trackers raises new challenges in terms of the design of the corresponding control and target motion estimation systems. The main challenge comes from the fact that communications among the trackers are constrained by the inter-tracker communication network, where trackers can only exchange information with their neighbors rather than

Algorithm 1 EKF for a single tracker

procedure INITIALIZATION

At $k=0$, initialize $\hat{\mathbf{x}}_{1|0}, P_{1|0}$

$\Omega_{1|0} = P_{1|0}^{-1}, \quad \mathbf{z}_{1|0} = P_{1|0}^{-1}\hat{\mathbf{x}}_{1|0}$

return $\hat{\mathbf{x}}_{1|0}, \Omega_{1|0}, \mathbf{z}_{1|0}$

At each discrete time k, repeat the following procedures:

procedure MEASUREMENT-UPDATE

if obtain a new range **then**

$C_k = \frac{\partial d_k}{\partial \mathbf{x}}(\hat{\mathbf{x}}_{k|k-1})$

$\tilde{y}_k = y_k - d_k(\hat{\mathbf{x}}_{k|k-1}) + C_k\hat{\mathbf{x}}_{k|k-1}$

Compute the innovation terms

$$\tilde{\mathbf{z}}_k = (C_k)^\top V \tilde{y}_k, \quad \tilde{\Omega}_k = (C_k)^\top V C_k. \tag{34}$$

else set $\tilde{\mathbf{z}}_k = \mathbf{0}, \tilde{\Omega}_k = 0$.

Correction

$$\mathbf{z}_{k|k} = \mathbf{z}_{k|k-1} + \tilde{\mathbf{z}}_k, \qquad \Omega_{k|k} = \Omega_{k|k-1} + \tilde{\Omega}_k \tag{35}$$

return $\mathbf{z}_{k|k}, \Omega_{k|k}, \hat{\mathbf{x}}_{k|k} = \Omega_{k|k}^{-1}\mathbf{z}_{k|k}$

procedure PREDICTION

$$\begin{aligned}\hat{\mathbf{x}}_{k+1|k} &= F\hat{\mathbf{x}}_{k|k}\\ \Omega_{k+1|k} &= Q - QF(\Omega_{k|k} + F^\top QF)^{-1}F^\top Q\end{aligned} \tag{36}$$

return $\hat{\mathbf{x}}_{k+1|k}, \Omega_{k+1|k}, \mathbf{z}_{k+1|k} = \Omega_{k+1|k}\hat{\mathbf{x}}_{k+1|k}$

with all trackers in the network. This requires that the design of control and estimation systems be addressed in a distributed manner.

A. Distributed estimation and control architecture

At the control level, the main objective is to design a distributed control system to drive the trackers along desired trajectories that i) ensure the observability of the target's motion and ii) maintain an optimal geometrical formation relative to the target with the objective of acquiring maximal range-information to estimate the target's state; see the characterization of such trajectories in Sections III-B.2 and III-B.3, and illustrations of optimal geometrical formations in Fig. III.1 for different numbers of trackers. Notice that there may exist multiple trajectories that satisfy conditions i) and ii). However, for the sake of simplicity, we inherit the methodology for the case of single tracker-single target presented in the previous section. That is, for each tracker i, a desired S-T curve, defined as

$$\mathbf{p}_{\mathrm{d}}^{[i]}(\gamma^{[i]}, t) = \mathbf{r}(\gamma^{[i]}) + \mathbf{q}(t), \tag{37}$$

is assigned for it to track, where $\mathbf{q}(t)$ is the target's trajectory and $\mathbf{r}^{[i]}(\cdot)$ is a corresponding spatial path encircling the target. This path is described by (15) and (16) for 3-D and 2-D cases, respectively, and parameterized by the variable $\gamma^{[i]}$ and the set of constant parameters $\{r_{\mathrm{x}}^{[i]}, r_{\mathrm{y}}^{[i]}, r_{\mathrm{z}}^{[i]}, \gamma_0^{[i]}\}$. It was explained in the previous section that if trackers can be controlled such that they converge to their corresponding S-T curves, then the pursuit task stated in Problem 1 will be fulfilled. In addition, with this design, if the paths $\mathbf{r}^{[i]}(\cdot); i \in \mathcal{V}$ are parameterized appropriately such that $\gamma_0^{[1]} - \gamma_0^{[2]} = \pi/2$ for $N = 2$ and $\gamma_0^{[i]} - \gamma_0^{[j]} = 2\pi/N$ for $N \geq 3$, where i, j are any two adjacent trackers, then the S-T curves will yield the desired geometrical formations relative to the target when $\gamma^{[i]} = \gamma^{[j]}$ for all $i, j \in \mathcal{V}$. In this context, $\gamma^{[i]}; i \in \mathcal{V}$ are called coordination states and the problem of coordinating the S-T curves to make the coordination states become equal (reach consensus) is called a coordination/consensus problem. This strategy borrows from the concepts of cooperative path following explained in [37]–[39]. See also the diagrams that illustrate the key concepts behind the design methodology in Fig. V.1.

With the new requirement on reaching an optimal geometrical formation relative to the target, the cooperative target pursuit problem stated in Problem 1, see (11), is re-stated as follows.

Problem 2 (Cooperative control for target pursuit): Consider the problem of cooperative target localization and pursuit stated in Problem 1. Supposed that each tracker is assigned a trajectory given by (37) *to track. Find control laws for the trackers' inputs* $\mathbf{u}^{[i]}$ *and for the evolution of the path parameters* $\dot{\gamma}^{[i]}$ *(or* $\ddot{\gamma}^{[i]}$*) to fulfill the following tasks:*

i Tracking:

$$\lim_{t\to\infty} \mathbf{p}_{\mathrm{d}}^{[i]}(\gamma^{[i]}(t), t) - \mathbf{p}^{[i]}(t) = \mathbf{0} \tag{38}$$

for all $i \in \mathcal{V}$.

ii Coordination (consensus):

$$\lim_{t\to\infty} \gamma^{[i]}(t) - \gamma^{[j]}(t) = 0, \tag{39a}$$

$$\lim_{t\to\infty} \dot{\gamma}^{[i]}(t) = \bar{\omega} \tag{39b}$$

for all $i, j \in \mathcal{V}$, *where* $\bar{\omega} \neq 0$ *is the common desired nominal angular speed assigned for the path parameters* $\gamma^{[i]}$ *for all* $i \in \mathcal{V}$.

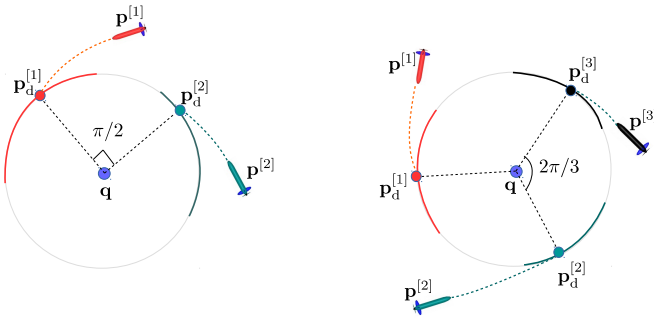

Fig. V.1: Design methodology for cooperative target pursuit. (Left: $N = 2$, Right: $N = 3$). Positions: $\mathbf{q}$ (target), $\mathbf{p}^{[i]}$ (trackers), and $\mathbf{p}_{\mathrm{d}}^{[i]}$ (desired hybrid PTs).

In order to solve the problem of cooperative target localization and pursuit while fulfilling the coordination requirement stated in (39), we propose a distributed estimation and control (DEC) system for each tracker $i; i \in \mathcal{V}$, as depicted in Fig.V.2. The underlying idea behind this architecture is briefly described as follows.

i) Cooperative Estimation: the main goal of this block is to solve the cooperative localization task given by (12) in a distributed manner. To this end, we adopt the distributed EKF (DEKF) methodology proposed in [24]. In the DEKF, the trackers exchange the local probability

density functions (PDFs) about the target's state and the innovation information obtained by local range measurements with their neighbors and apply a fusion (consensus) algorithm. As a result of this cooperative process, the estimates of the target's state reach consensus and are potentially more accurate than that obtained in the case each tracker estimates the target's state by itself (non-cooperative strategy).

ii) Cooperative Control: the main goal of this block is to solve the coordination task given by (39) by using a distributed coordination/consensus control law that computes correction speeds $v_c^{[i]}; i \in \mathcal{V}$ about the nominal speed $\bar{\omega}$ to coordinate the path parameters and make them reach consensus. The control law for $v_c^{[i]}$ uses local information $(\gamma^{[i]})$ (and possibly $\dot{\gamma}^{[i]}$) and information from its in-neighboring trackers $(\gamma^{[j]}, \dot{\gamma}^{[j]}; j \in \mathcal{N}_{\text{in}}^{[i]})$. For this reason, the trackers are required to communicate and exchange the corresponding path variables $\gamma^{[i]}$ (and possibly $\dot{\gamma}^{[i]}$) with theirs neighbors.

iii) Tracking Controller: this controller aims to make the trackers converge to and follow their assigned trajectorys given by (37), i.e. solve the tracking task given by (38). To track the trajectories, the tracking controllers developed in previous section will be used with a sightly modification that takes into account the cooperative information provided by the cooperative layer.

The design of the complete DEC system is described next.

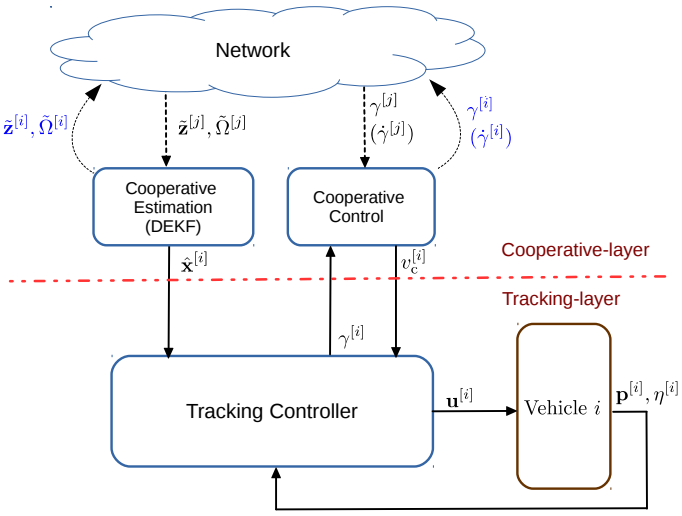

Fig. V.2: The DEC system as seen by tracker i. In the figure, $j \in \mathcal{N}_{\text{in}}^{[i]}$.

B. Cooperative estimation

In this section, we propose a DEKF that solves the cooperative estimation problem defined by (12). The design of the DEKF borrows from the work in [24] and is described next. Let $Y_k^{[i]} \triangleq \{y_m^{[i]}\}_{m=0}^k$ denote the set of ranges to the target measured by tracker $i; i \in \mathcal{V}$ and $\mathcal{I}_k^{[j]}; j \in \mathcal{N}_{\text{in}}^{[i]}$ the collective information (PDFs of the target's state estimated by its in-neighboring trackers) that the tracker has received up to time k. Let also

$$p^{[i]}(\mathbf{x}_k|Y_{k-1}^{[i]}, \mathcal{I}_{k-1}^{[j]}) \sim \mathcal{N}(\hat{\mathbf{x}}_{k|k-1}^{[i]}, P_{k|k-1}^{[i]}), \tag{40a}$$

$$p^{[i]}(\mathbf{x}_k|Y_k^{[i]}, \mathcal{I}_k^{[j]}) \sim \mathcal{N}(\hat{\mathbf{x}}_{k|k}^{[i]}, P_{k|k}^{[i]}) \tag{40b}$$

be the prior and posterior PDF of the target's state, respectively, estimated at time k by tracker i. Let also $\mathbf{z}^{[i]}$ and $\Omega^{[i]}$ denote the corresponding information vector and information matrix, respectively, as defined by (33).

The proposed DEKF for cooperative target localization is described in Algorithm 2, organized in a series of procedures. Compared with Algorithm 1, there are two key procedures, namely, "Communication" and "Fusion", that must be implemented prior to the "Prediction" procedure. The "Communication" procedure is used to transmit the latest local PDF about the target estimated by each tracker to its out-neighbors. The "Fusion" procedure is implemented to fuse, at the level of each tracker, the local corrected PDF about the target's state with the PDFs received from the neighbors. This is done to improve the accuracy of the target 's state estimate and also to ensure that consensus is reached on the estimates of the target's state. This procedure can be implemented using (43). Note that in these equations, $\pi^{[i,j]}; i \in \mathcal{V}, j \in \mathcal{N}_{\text{in}}^{[i]} \cup \{i\}$ are weighting parameters that must be chosen such that $\pi^{[i,j]} > 0$ and $\sum_{j \in \mathcal{N}_{\text{in}}^{[i]} \cup \{i\}} \pi^{[i,j]} = 1$ for all $i \in \mathcal{V}$. The prediction step is done similarly to the case of single tracker, computed by (44). Similar to Algorithm 1, $V^{[i]}$ is normally chosen as the covariance matrix of the range measurement noise. That is, $V^{[i]} = \sigma$ for all $i \in \mathcal{V}$.

Remark 7: Algorithm 1 is a special case of Algorithm 2 with $N = 1$.

Remark 8: For the sake of simplicity and in order to save on communications, at each sampling period Algorithm 2 requires that the trackers exchange information with their neighbors only one time in order to update the "Fusion" step. This is equivalent to setting $L = 1$ in [24], where L is the number of interactions among the trackers during each sampling interval $[k, k+1]$ used to fuse the information about the estimated target's state. The larger the number L, the faster will the convergence of the DEKF be; however, more communications will be required among the trackers [24].

C. Cooperative target pursuit

We now propose controllers for each tracker i to solve the problem of cooperative control for target pursuit stated in Problem 2. Inspired by the work in the field of consensus of multi agent systems [40], at the cooperative control level, a distributed control law for the correction speed $v_c^{[i]}$ in a form of consensus protocol is given as

$$v_c^{[i]} = -k_c \sum_{j \in \mathcal{N}_{\text{in}}^{[i]}} (\gamma^{[i]} - \gamma^{[j]}), \tag{45}$$

where $k_c > 0$ is a coupling gain. With this correction speed, the total desired speed that for $\gamma^{[i]}$ to track is given by

$$\omega_d^{[i]} = \bar{\omega} + v_c^{[i]}, \tag{46}$$

Algorithm 2 Distributed EKF for tracker i

procedure INITIALIZATION

At $k=0$, initialize $\hat{\mathbf{x}}_{1|0}^{[i]}, P_{1|0}^{[i]}$

$\Omega_{1|0}^{[i]} = [P_{1|0}^{[i]}]^{-1}, \quad \mathbf{z}_{1|0}^{[i]} = [P_{1|0}^{[i]}]^{-1}\hat{\mathbf{x}}_{1|0}^{[i]}$

return $\hat{\mathbf{x}}_{1|0}^{[i]}, \Omega_{1|0}^{[i]}, \mathbf{z}_{1|0}^{[i]}$

At each discrete time k, repeat the following procedures:

procedure CORRECTION

if obtain a new range **then**

$$C_k^{[i]} = \frac{\partial d_k^{[i]}}{\partial \mathbf{x}}(\hat{\mathbf{x}}_{k|k-1}^{[i]})$$

$$\tilde{y}_k^{[i]} = y_k^{[i]} - d_k^{[i]}(\hat{\mathbf{x}}_{k|k-1}^{[i]}) + C_k^{[i]}\hat{\mathbf{x}}_{k|k-1}^{[i]}$$

$$\begin{aligned}\tilde{\mathbf{z}}_k^{[i]} &= \mathbf{z}_{k|k-1}^{[i]} + (C_k^{[i]})^\top V^{[i]}\tilde{y}_k^{[i]} \\ \tilde{\Omega}_k^{[i]} &= \Omega_{k|k-1}^{[i]} + (C_k^{[i]})^\top V^{[i]} C_k^{[i]}\end{aligned} \tag{41}$$

else set $\tilde{\mathbf{z}}_k^{[i]} = \mathbf{z}_{k|k-1}^{[i]}, \tilde{\Omega}_k^{[i]} = \Omega_{k|k-1}^{[i]}$.

procedure COMMUNICATION

Transmit to its out-neighbors a message $\mathcal{M}_{\rm e}(k)$, defined as

$$\mathcal{M}_{\rm e}(k) \triangleq \{\tilde{\mathbf{z}}_k^{[i]}, \tilde{\Omega}_k^{[i]}\} \tag{42}$$

procedure FUSION (CONSENSUS ESTIMATION)

$$\begin{aligned}\mathbf{z}_{k|k}^{[i]} &= \sum_{j\in\mathcal{N}_{\rm in}^{[i]}\cup\{i\}} \pi^{[i,j]}\tilde{\mathbf{z}}_k^{[j]} \\ \Omega_{k|k}^{[i]} &= \sum_{j\in\mathcal{N}_{\rm in}^{[i]}\cup\{i\}} \pi^{[i,j]}\tilde{\Omega}_k^{[j]}\end{aligned} \tag{43}$$

return $\mathbf{z}_{k|k}^{[i]}, \Omega_{k|k}^{[i]}, \hat{\mathbf{x}}_{k|k}^{[i]} = [\Omega_{k|k}^{[i]}]^{-1}\mathbf{z}_{k|k}^{[i]}$

procedure PREDICTION

$$\begin{aligned}\hat{\mathbf{x}}_{k+1|k}^{[i]} &= F\hat{\mathbf{x}}_{k|k}^{[i]} \\ \Omega_{k+1|k}^{[i]} &= Q - QF(\Omega_{k|k}^{[i]} + F^\top QF)^{-1}F^\top Q\end{aligned} \tag{44}$$

return $\hat{\mathbf{x}}_{k+1|k}^{[i]}, \Omega_{k+1|k}^{[i]}, \mathbf{z}_{k+1|k}^{[i]} = \Omega_{k+1|k}^{[i]}\hat{\mathbf{x}}_{k+1|k}^{[i]}$

where as explained before, $\bar{\omega}$ is the nominal desired speed for all $\gamma^{[i]}; i \in \mathcal{V}$. Similarly to (20), define also

$$e_\gamma^{[i]} = \dot{\gamma}^{[i]} - \omega_{\rm d}^{[i]} \tag{47}$$

as the speed tracking error for the evolution of $\gamma^{[i]}$ for each tracker $i; i \in \mathcal{V}$. Similar to (27), let

$$\hat{\mathbf{e}}_{\rm p}^{[i]} = R^\top(\boldsymbol{\eta}^{[i]})\left(\mathbf{p}^{[i]} - \mathbf{r}(\gamma^{[i]}) - \hat{\mathbf{q}}^{[i]}\right) - \boldsymbol{\epsilon}. \tag{48}$$

To track the trajectory we adopt the tracking controllers given by (28) and (29) for each tracker $i; i \in \mathcal{V}$ as follows.

Tracking Controller - Type I

$$\mathbf{u}^{[i]} = \boldsymbol{k}(\hat{\mathbf{x}}^{[i]}) \tag{49a}$$

$$\dot{\gamma}^{[i]} = \omega_{\rm d}^{[i]}. \tag{49b}$$

Tracking Controller - Type II

$$\mathbf{u}^{[i]} = \boldsymbol{k}(\hat{\mathbf{x}}^{[i]}) \tag{50a}$$

$$\ddot{\gamma}^{[i]} = -k_\gamma e_\gamma^{[i]} + (\hat{\mathbf{e}}_{\rm p}^{[i]})^\top R^\top(\boldsymbol{\eta}^{[i]})\mathbf{r}'(\gamma^{[i]}) + \dot{v}_{\rm c}^{[i]}, \tag{50b}$$

where in (49) and (50)

$$\boldsymbol{k}(\hat{\mathbf{x}}^{[i]}) = \bar{\Delta}\left(R^\top(\boldsymbol{\eta}^{[i]})\left(\mathbf{r}'(\gamma^{[i]})\omega_{\rm d}^{[i]} + \hat{\boldsymbol{v}}^{[i]}\right) - K_{\rm p}\hat{\mathbf{e}}_{\rm p}^{[i]}\right) \tag{51}$$

and in (50)

$$\dot{v}_c^{[i]} = -k_c \sum_{j\in\mathcal{N}_{\rm in}^{[i]}} (\dot{\gamma}^{[i]} - \dot{\gamma}^{[j]}), \tag{52}$$

with $\omega_{\rm d}^{[i]}, e_\gamma^{[i]}$ and $\hat{\mathbf{e}}_{\rm p}^{[i]}$ are given by (46)–(48).

Remark 9: Both types of controllers require the trackers to exchange the coordination state $\gamma^{[i]}; i \in \mathcal{V}$ to compute the correction speed $v_{\rm c}^{[i]}$. However, Tracking Controller-Type II in (50) *also requires the trackers to exchange $\dot{\gamma}^{[i]}; i \in \mathcal{V}$ (in order to compute $\dot{v}_c^{[i]}$) .*

D. Stability analysis of the complete DEC system

We now show that the proposed DEC system designed in Sections V-B and V-C solves the cooperative target localization and pursuit problem while verifying a robust stability property. To this end, we analyze the convergence of estimation, coordination, and pursuit errors of the complete DEC system, defined as follows.

1) Estimation error: Let

$$\tilde{\mathbf{x}}^{[i]} \triangleq \hat{\mathbf{x}}^{[i]} - \mathbf{x}. \tag{53}$$

be the estimation error of the target's state estimated by tracker $i; i \in \mathcal{V}$. Collectively, the total estimation error of the complete DEC system is defined as

$$\tilde{\mathbf{x}} \triangleq \text{col}\left(\tilde{\mathbf{x}}^{[1]}, ..., \tilde{\mathbf{x}}^{[N]}\right) \in \mathbb{R}^{nN}. \tag{54}$$

2) Coordination error: Recall that with the proposed methodology, the path parameters $\gamma^{[i]}$ represent the coordination states of the trackers. Let

$$\xi_i = \gamma^{[i]} - \sum_{j=1}^{N} r_j\gamma^{[j]} \tag{55}$$

be the coordination error among the trackers, where r_i is the $i^{\rm th}$ component of the left eigenvector of the Laplacian matrix of the underlying communication graph. Note also that if the graph is balanced, then $\mathbf{r} = \mathbf{1}/N$ where recall that $\mathbf{1} \in \mathbb{R}^N, \mathbf{1} = [1]_{N\times 1}$. In this case, ξ_i measures the disagreement between the coordination state $\gamma^{[i]}$ and the average of all coordination states. Let also $\boldsymbol{\xi} \triangleq [\xi_1^\top, ..., \xi_N^\top]^\top \in \mathbb{R}^N$ be the coordination error vector that captures the disagreement among the coordination states. From (55), $\boldsymbol{\xi}$ can be rewritten as

$$\boldsymbol{\xi} = W\boldsymbol{\gamma}, \tag{56}$$

where $\boldsymbol{\gamma} \triangleq [\gamma^{[1]}, ..., \gamma^{[N]}]^\top \in \mathbb{R}^N$ and

$$W \triangleq I_N - \mathbf{1}\mathbf{r}^\top. \tag{57}$$

With the above definition, it is clear that all coordination states are synchronized, that is, $\gamma^{[1]} = \gamma^{[2]} = ... = \gamma^{[N]}$ if and only if $\boldsymbol{\xi} = \mathbf{0}$. Therefore, to analyze consensus of the coordination

states, we analyze the convergence of the coordination error $\boldsymbol{\xi}$ to zero. The dynamics of $\boldsymbol{\xi}$ are given by

$$\begin{aligned}\dot{\boldsymbol{\xi}} &= W\dot{\boldsymbol{\gamma}} \overset{(45)-(47)}{=} W(\mathbf{1}\bar{\omega} + -k_c L\boldsymbol{\gamma} + \mathbf{e}_\gamma)\\ &= -k_c L\boldsymbol{\xi} + W\mathbf{e}_\gamma \\ &\triangleq \mathbf{f}_1(\boldsymbol{\xi}, \mathbf{e}),\end{aligned} \tag{58}$$

where $\mathbf{e}_\gamma \triangleq [e_\gamma^{[1]}, ..., e_\gamma^{[N]}]^\top \in \mathbb{R}^N$. Above we used Lemma 1 for the last equality, that is, because $\mathbf{r}^\top \mathbf{1} = 1$ and $\mathbf{r}^\top L = 0$; therefore, $W\mathbf{1} = \mathbf{0}$ and $WL = LW$.

3) Pursuit error: Similarly to (19), let

$$\mathbf{e}_{\mathrm{p}}^{[i]} = R^\top(\boldsymbol{\eta}^{[i]})(\mathbf{p}^{[i]} - \mathbf{r}(\gamma^{[i]}) - \mathbf{q}) - \boldsymbol{\epsilon} \tag{59}$$

be the position error between tracker i and the vicinity of the target. From (48) and (59) it follows that

$$\hat{\mathbf{e}}_{\mathrm{p}}^{[i]} = \mathbf{e}_{\mathrm{p}}^{[i]} - R^\top(\boldsymbol{\eta}^{[i]})\tilde{\mathbf{q}}^{[i]}, \tag{60}$$

where $\tilde{\mathbf{q}}^{[i]} \triangleq \hat{\mathbf{q}}^{[i]} - \mathbf{q}^{[i]}$ is the the estimation error of the the target's position, estimated by tracker i. The dynamics of the error can be obtained similarly to (21) as

$$\dot{\mathbf{e}}_{\mathrm{p}}^{[i]} = -S(\boldsymbol{\omega}^{[i]})\mathbf{e}_{\mathrm{p}}^{[i]} + \Delta\mathbf{u}^{[i]} - R^\top(\boldsymbol{\eta}^{[i]})\left(\mathbf{r}'(\gamma^{[i]})\dot{\gamma}^{[i]} + \boldsymbol{v}\right)$$

Note that the control law for $\mathbf{u}^{[i]}$ is identical for two types of tracking controllers (49) and (50). Thus, making $\mathbf{u}^{[i]} = \boldsymbol{k}(\hat{\mathbf{x}}^{[i]})$, where $\boldsymbol{k}(\hat{\mathbf{x}}^{[i]})$ given by (51) and using the relation in (47) in the above equation, we obtain

$$\begin{aligned}\dot{\mathbf{e}}_{\mathrm{p}}^{[i]} = &- S(\boldsymbol{\omega}^{[i]})\mathbf{e}_{\mathrm{p}}^{[i]} + R^\top(\boldsymbol{\eta}^{[i]})\left(\tilde{\boldsymbol{v}}^{[i]} - \mathbf{r}'(\gamma^{[i]})e_\gamma^{[i]}\right)\\ &- K_{\mathrm{p}}\left(\mathbf{e}_{\mathrm{p}}^{[i]} - R^\top(\boldsymbol{\eta}^{[i]})\tilde{\mathbf{q}}^{[i]}\right),\end{aligned} \tag{61}$$

where $\tilde{\boldsymbol{v}}^{[i]} \triangleq \hat{\boldsymbol{v}}^{[i]} - \boldsymbol{v}^{[i]}$ is the estimation error of the target's velocity, estimated by tracker i.

We now derive the dynamics for $e_\gamma^{[i]}$ defined by (47). For the Tracking-Controller Type I given by (49), $e_\gamma^{[i]} = 0$, hence $\dot{e}_\gamma^{[i]}(t) = 0$ for all t and $i \in \mathcal{V}$. For the Tracking-Controller Type II, the dynamics of $e_\gamma^{[i]}$ are given by

$$\dot{e}_\gamma^{[i]} \overset{(46),(47)}{=} \ddot{\gamma}^{[i]} - \dot{v}_{\mathrm{c}}^{[i]}$$

Substituting $\ddot{\gamma}^{[i]}$ in (50b) in the above equation yields

$$\dot{e}_\gamma^{[i]} = -k_\gamma e_\gamma^{[i]} + \hat{\mathbf{e}}_{\mathrm{p}}^\top R^\top(\boldsymbol{\eta})\mathbf{r}'(\gamma). \tag{62}$$

Let also $\mathbf{e}^{[i]} = [(\mathbf{e}_{\mathrm{p}}^{[i]})^\top, e_\gamma^{[i]}]^\top$ be the tracking error vector of tracker i. Collectively, the pursuit error of the complete DEC system is defined as

$$\mathbf{e} \triangleq \mathrm{col}(\mathbf{e}^{[1]}, ..., \mathbf{e}^{[N]}). \tag{63}$$

From (61) and (62), the dynamics of the total pursuit error can be rewritten in the general form

$$\dot{\mathbf{e}} = \mathbf{f}_2(\mathbf{e}, \tilde{\mathbf{x}}, \boldsymbol{\xi}). \tag{64}$$

We now study the stability of the complete DEC system by analyzing the inter-connected system consisting of the systems (58) and (64), see Fig.V.3. First, we analyze the stability of each sub-system as follows

Lemma 3 (stability of the coordination system): Consider the coordination error system described by (58)*. Assume further that the communication digraph is strongly connected. Then, the coordination error system is ISS with respect to the state* $\boldsymbol{\xi}$ *and the input* $\mathbf{e}$*.*

Proof: See the Appendix

Lemma 4 (stability of the pursuit error system): Consider the complete pursuit error system described by (64)*. Then, the complete tracking error system is ISS with respect to the state* $\mathbf{e}$ *and the input* $\tilde{\mathbf{x}}$*, where* $\tilde{\mathbf{x}}$ *is the total estimation error of the target state given by* (54) *.*

Proof. See the Appendix.

Remark 10: Lemma 4 implies that with tracking controllers given in (49) *and* (50)*, the tracking error system is independent of the correction speed* $v_{\mathrm{c}}^{[i]}$*.*

Theorem 2: Consider the closed-loop complete DEC system composed by the coordination error system (58) *and the pursuit error system* (64)*. Let assumptions in Lemma 3 and Lemma 4 hold. Then, the complete DEC system is ISS respect to the state* $\boldsymbol{\mu} \triangleq [\boldsymbol{\xi}^\top, \mathbf{e}^\top]^\top$ *and the input* $\tilde{\mathbf{x}}$*, where* $\tilde{\mathbf{x}}$ *is the total estimation error of the target state given by* (54)*.*

Theorem 2 follows immediately from Lemma 3 and Lemma 4 and the stability of cascaded ISS systems [41]. The ISS property of the close-looped DEC system implies that the pursuit and coordination error ($\boldsymbol{\mu}$) depend only on the estimation error of the target' state ($\tilde{\mathbf{x}}$) generated by the DEKF and is robust against this error in the sense that as long as $\tilde{\mathbf{x}}$ is bounded, then $\boldsymbol{\mu}$ is bounded. Furthermore, if $\tilde{\mathbf{x}}$ converges zero then $\boldsymbol{\mu}$ converges to zero as well. According to [24], provided that the digraph induced by the tracker's network is strongly connected and the initial estimates of the target's state are sufficiently close to the true target, then $\tilde{\mathbf{x}}$ is guaranteed to be bounded and asymptotically converge to a ball whose size depends on the size of the covariances of range measurement and process noises. Note that this requirement on the connectivity of network is satisfied with Lemma 3, whereas the requirement on the initial estimates is standard with EKF.

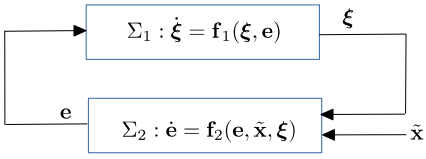

Fig. V.3: The closed-loop DEC system.

VI. SIMULATION EXAMPLES

Animation videos of the simulation results can be found at:

- 2D-1 Tracker: `https://youtu.be/nYfQvMq_RRo`
- 2D-3 Trackers: `https://youtu.be/J94cYoKW4y0`
- 3D-1 Tracker: `https://youtu.be/jbJOe6ppwDg`
- 3D-3 Trackers: `https://youtu.be/YuWicw6N9qc`

In this section, we will present simulation results that illustrate the performance of the DEC in pursuing and localizing a target. We consider two scenarios: the first with one tracker ($N = 1$) and the second with three trackers ($N = 3$). With $N = 3$, the communication topology adopted is depicted in Fig. VI.1, which shows the indexes of the trackers and

the directional communication links among them (represented by arrows). The simulation parameters for the 2-D and 3-D cases are given in Table I and Table II, respectively. In all simulations the sampling interval for range measurements is 2 seconds and the Tracking Controller-Type II was used.

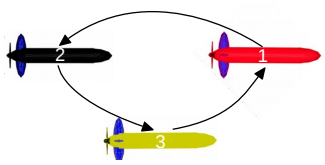

Fig. VI.1: The communication network of three trackers. Arrows indicate directions of the information flow, thus inducing a directed graph.

A. 2-D-cases

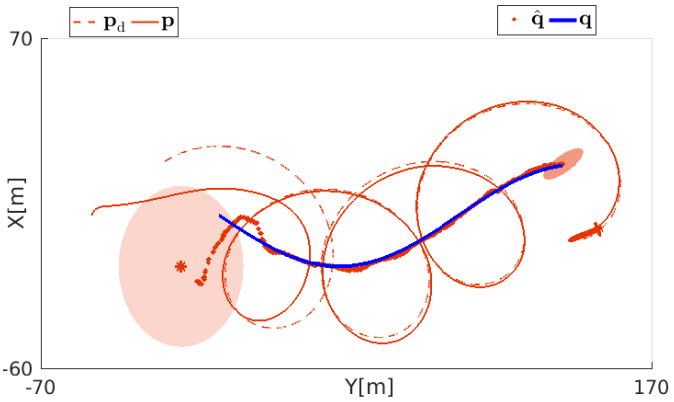

a) One tracker ($N = 1$)

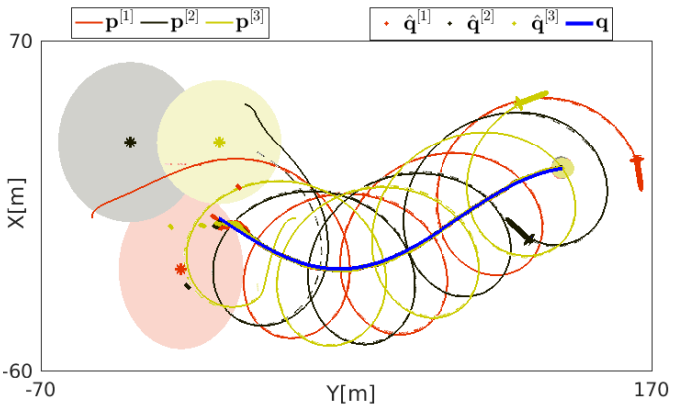

b) Three trackers ($N = 3$).

Fig. VI.2: 2-D cases: The filled ellipsoids represent the uncertainties (covariances) of the target's position estimated by the trackers at the beginning and end of the simulation. Trajectories. $\mathbf{p}^{[i]}$: trackers, $\mathbf{p}_d^{[i]}$: desired path, $\mathbf{q}$: target, $\hat{\mathbf{q}}^{[i]}$: estimated target.

The performance of the DEC strategy for localizing and pursuing the target in 2-D using one tracker and three trackers are plotted in Fig.VI.2 and Fig.VI.3. Fig.VI.2 (a) shows that in both scenarios the trackers converge to and stay in the vicinity of the target, and encircle the latter. The figure also indicates that the target's positions estimated by the trackers converge to a small neighborhood of the true target's position. This can be verified by observing Fig.VI.3 where it is evident that the pursuit errors and the localization errors converge nearly to zero, implying that both the pursuit and localization tasks are fulfilled.

Fig.VI.3 also indicates that with three trackers, the convergence of the pursuit and the localization errors is faster than that obtained using only Tracker 1. Fig.VI.2(b) also shows that the uncertainty regions of the target' position estimated by the three trackers (computed from the covariance matrices $P^{[i]}$ and represented by the ellipsoids) converge to almost the same size, which is smaller than the size of the uncertainty region of the target' position estimated using only Tracker 1.

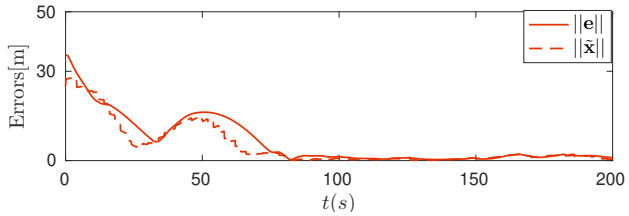

a) One tracker ($N = 1$).

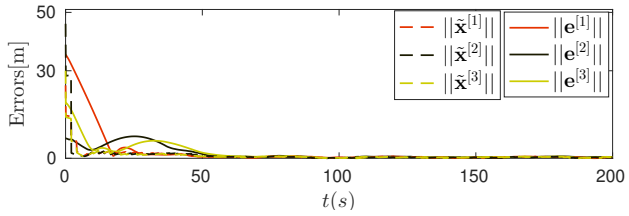

b) There trackers ($N = 3$)

Fig. VI.3: 2-D cases: Pursuit errors ($\left\|\mathbf{e}^{[i]}\right\|$) and localization errors ($\left\|\tilde{\mathbf{x}}^{[i]}\right\|$), $i = 1, 2, 3$.

Fig. VI.4 shows the performance of the coordination system. It is visible that all the path parameters reach consensus and evolve with the common desired speed $\bar{\omega}$. This implies that the trackers converge to and maintain in the desired formation that allows them to acquire maximal range information to estimate the target's state.

Remark 11: Note that in the case of multiple trackers, it would be more efficient in terms of energy consumption if the trackers move alongside the target's trajectory, instead of rotating around the target. With the proposed strategy this can be done by setting $\bar{\omega} = 0$. We simulated this situation and the result can be visualized at `https://youtu.be/swNsGShS7gM`. *However, if only one tracker is used to localize the target then moving translationally with the target's trajectory does not grantee observability of the target, see observability analysis in [18].*

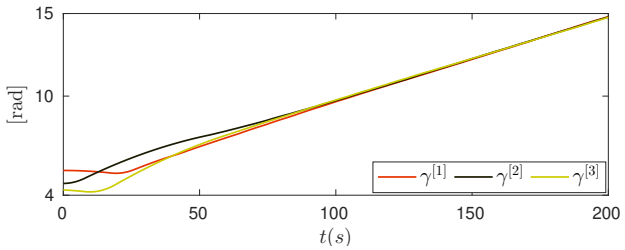

a) Evolution of the path parameters

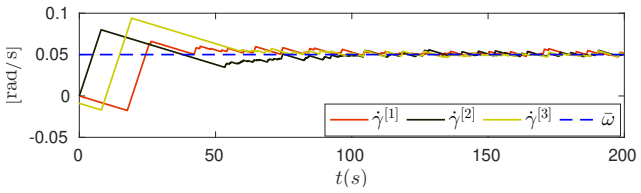

b) Speeds of the path parameters

Fig. VI.4: 2-D cases. Coordination performance in case with three trackers ($N = 3$).

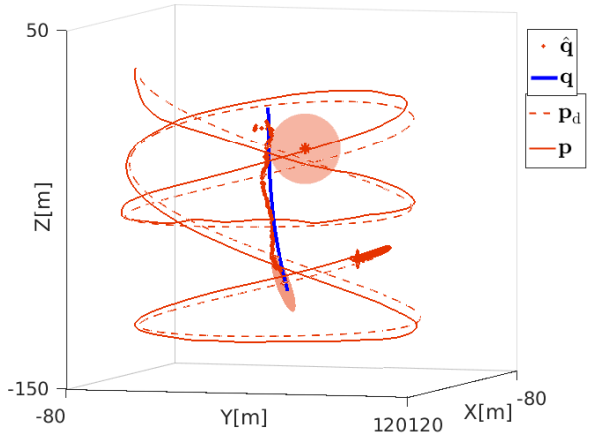

a) One tracker ($N = 1$).

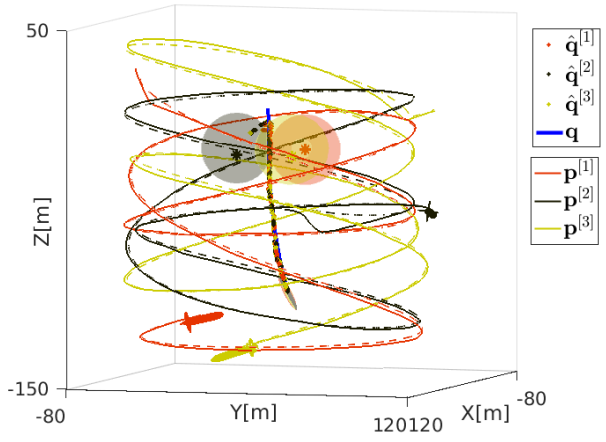

b) Three trackers ($N = 3$).

Fig. VI.5: 3-D cases: The filled ellipsoids represent the uncertainties (covariances) of the target's position estimated by the trackers at the beginning and the end of the simulation. Trajectories. $\mathbf{p}^{[i]}$: trackers, $\mathbf{q}$: target, $\hat{\mathbf{q}}^{[i]}$: estimated target.

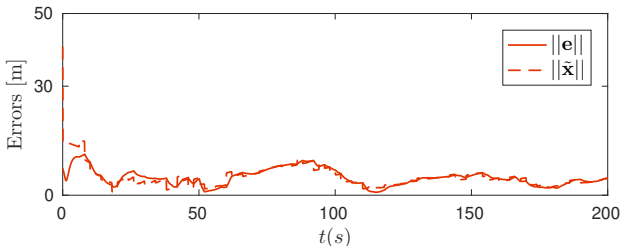

a) One tracker ($N = 1$).

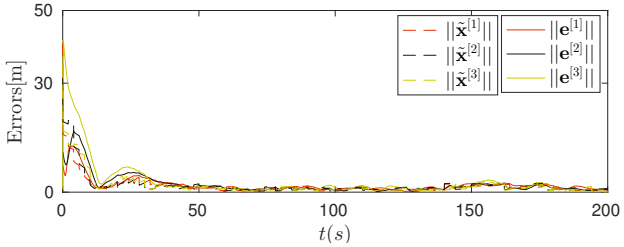

b) Three trackers ($N = 3$).

Fig. VI.6: 3-D cases: Pursuit errors ($\left\|\mathbf{e}^{[i]}\right\|$) and localization errors ($\left\|\tilde{\mathbf{x}}^{[i]}\right\|$), $i = 1, 2, 3$.

B. 3-D-cases

The performance of the DEC strategy for 3-D cases is illustrated in Fig.VI.5 and Fig.VI.6. The figures show that the pursuit and localization errors are bounded and converge nearly to zero in both scenarios. However, Fig.VI.6 indicates that the errors converge faster, and asymptotically are smaller with three trackers. Fig. VI.7 shows the performance of the coordination system in the case of there trackers. It is visible that all the path parameters reach consensus and evolve with the common desired speed $\bar{\omega}$. This implies that the coordination task is fulfilled as well.

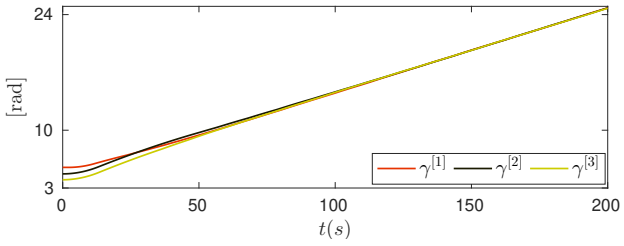

a) Evolution of the path parameters

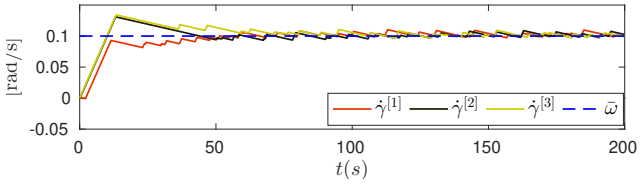

b) Speeds of the path parameters

Fig. VI.7: 3-D cases. Coordination performance in case with three trackers ($N = 3$).

VII. CONCLUSIONS

We proposed an integrated motion planning, control, and estimation framework to solve the problem of range-based simultaneous target localization and pursuit using one or multiple autonomous trackers. At the motion planning level, optimal tracker-target geometrical formations for target localization purposes were derived that led naturally to the concept of S-T curves with a hybrid temporal-spatial parameterization that serve as references for the desired motion of the trackers. This was followed by the derivation of two robust tracking controllers for S-T curve tracking. In the case of multiple trackers, an efficient distributed cooperative estimation and control strategy was proposed to deal with the constraints imposed by the inter-tracker communication network topology. The results of extensive simulations showed the robustness and efficacy of the proposed method. Stability analysis showed that the performance of the complete DEC system depends only on the convergence the EKF (DEKF for the case of multiple trackers) which, in practice, requires proper initialization of the estimated target's state and covariances. Future work aims at extending the proposed method to the case of multiple targets, with the main focus on multiple tracker motion planning.

REFERENCES

[1] C. M. Clark, C. Forney, E. Manii, D. Shinzaki, C. Gage, M. Farris, C. G. Lowe, and M. Moline. Tracking and following a tagged leopard shark with an autonomous underwater vehicle. *Journal of Field Robotics*, 30(3):309–322, 2013.

[2] A. Zolich, T. A. Johansen, J. A. Alfredsen, J. Kuttenkeuler, and E. Erstorp. A formation of unmanned vehicles for tracking of an acoustic fish-tag. In *OCEANS 2017 - Anchorage*, pages 1–6, Sep. 2017.

[3] L. Philippe, H. Jean-Philippe, M. Jean-Claude, and Eric N. Air and spaceborne radar systems: An introduction. William Andrew Publishing, Norwich, NY, 2001.

[4] B. Ristic, S. Arulampalam, and N. Gordon. *Beyond the Kalman filter: particle filters for tracking applications*. Artech House, 2004.

[5] Nguyen T. Hung, N. Crasta, David Moreno-Salinas, António M. Pascoal, and Tor A. Johansen. Range-based target localization and pursuit with autonomous vehicles: An approach using posterior CRLB and model predictive control. *Robotics and Autonomous Systems*, 132:103608, 2020.

[6] N. Crasta, D. Moreno-Salinas, B. Bayat, A. M. Pascoal, and J. Aranda. Range-based underwater target localization using an autonomous surface vehicle: Observability analysis. In *2018 IEEE/ION Position, Location and Navigation Symposium (PLANS)*, pages 487–496, April 2018.

[7] K. Vickery. Acoustic positioning systems. a practical overview of current systems. In *Proceedings of the 1998 Workshop on Autonomous Underwater Vehicles (Cat. No.98CH36290)*, pages 5–17, Aug 1998.

[8] Hwee-Pink Tan, Roee Diamant, Winston K.G. Seah, and Marc Waldmeyer. A survey of techniques and challenges in underwater localization. *Ocean Engineering*, 38(14):1663 – 1676, 2011.

[9] Iman Shames, Baris Fidan, and Brian D. O. Anderson. Close target reconnaissance using autonomous uav formations. In *2008 47th IEEE Conference on Decision and Control*, pages 1729–1734, 2008.

[10] Pedro Batista, Carlos Silvestre, and Paulo Oliveira. Single range aided navigation and source localization: Observability and filter design. *Systems and Control Letters*, 60(8):665 – 673, 2011.

[11] D. Pillon, A. Perez-Pignol, and C. Jauffret. Observability: range-only vs. bearings-only target motion analysis for a leg-by-leg observer's trajectory. *IEEE Transactions on Aerospace and Electronic Systems*, 52(4):1667–1678, August 2016.

[12] C. Jauffret, A. Pérez, and D. Pillon. Observability: Range-only versus bearings-only target motion analysis when the observer maneuvers smoothly. *IEEE Transactions on Aerospace and Electronic Systems*, 53(6):2814–2832, Dec 2017.

[13] F. Arrichiello, G. Antonelli, A. Aguiar, and A. Pascoal. An observability metric for underwater vehicle localization using range measurements. *Sensors*, 13(12):16191–16215, 2013.

[14] G. Indiveri, P. Pedone, and M. Cuccovillo. Fixed target 3d localization based on range data only: a recursive least squares approach. *IFAC Proceedings Volumes*, 45(5):140 – 145, 2012. 3rd IFAC Workshop on Navigation, Guidance and Control of Underwater Vehicles.

[15] I. Masmitja, S. Gomariz, J. Del-Rio, B. Kieft, T. O'Reilly, P. J Bouvet, and J. Aguzzi. Optimal path shape for range-only underwater target localization using a wave glider. *The International Journal of Robotics Research*, 37(12):1447–1462, 2018.

[16] B. Ristic, S. Arulampalam, and J. McCarthy. Target motion analysis using range-only measurements: algorithms, performance and application to ISAR data. *Signal Processing*, 82(2):273 – 296, 2002.

[17] N. Crasta, D. Moreno-Salinas, A.M. Pascoal, and J. Aranda. Multiple autonomous surface vehicle motion planning for cooperative range-based underwater target localization. *Annual Reviews in Control*, 46:326 – 342, 2018.

[18] Nguyen T. Hung and Antonio M. Pascoal. Range-based navigation and target localization: Observability analysis and guidelines for motion planning. *IFAC-PapersOnLine*, 53(2):14620–14627, 2020. 21th IFAC World Congress.

[19] Iman Shames, Soura Dasgupta, Barış Fidan, and Brian D. O. Anderson. Circumnavigation using distance measurements under slow drift. *IEEE Transactions on Automatic Control*, 57(4):889–903, 2012.

[20] Barış Fidan, Soura Dasgupta, and Brian D.O. Anderson. Adaptive range-measurement-based target pursuit. *International Journal of Adaptive Control and Signal Processing*, 27(1-2):66–81, 2013.

[21] F. Koohifar, I. Guvenc, and M. L. Sichitiu. Autonomous tracking of intermittent RF source using a UAV swarm. *IEEE Access*, 6:15884–15897, 2018.

[22] Gaurav Chaudhary, Arpita Sinha, Twinkle Tripathy, and Aseem Borkar. Conditions for target tracking with range-only information. *Robotics and Autonomous Systems*, 75:176 – 186, 2016.

[23] T. Nguyen, Z. Qiu, M. Cao, T. H. Nguyen, and L. Xie. An integrated localization-navigation scheme for distance-based docking of UAVs. In *2018 IEEE/RSJ International Conference on Intelligent Robots and Systems (IROS)*, pages 5245–5250, 2018.

[24] Giorgio Battistelli and Luigi Chisci. Stability of consensus extended Kalman filter for distributed state estimation. *Automatica*, 68:169 – 178, 2016.

[25] Marcello Farina, Giancarlo Ferrari-Trecate, and Riccardo Scattolini. Distributed moving horizon estimation for nonlinear constrained systems. *International Journal of Robust and Nonlinear Control*, 22(2):123–143, 2012.

[26] Isaac L. Manuel and Adrian N. Bishop. Distributed Monte Carlo information fusion and distributed particle filtering. *IFAC Proceedings Volumes*, 47(3):8681 – 8688, 2014. 19th IFAC World Congress.

[27] Francisco F.C. Rego, António M. Pascoal, A. Pedro Aguiar, and Colin N. Jones. Distributed state estimation for discrete-time linear time invariant systems: A survey. *Annual Reviews in Control*, 48:36 – 56, 2019.

[28] W. Yu, G. Chen, M. Cao, and J. Kurths. Second-order consensus for multiagent systems with directed topologies and nonlinear dynamics. *IEEE Transactions on Systems, Man, and Cybernetics, Part B (Cybernetics)*, 40(3):881–891, June 2010.

[29] Z. Li and Z. Duan. *Cooperative Control of Multi-Agent Systems*. CRC Press, 2015.

[30] Pedro Caldeira Abreu, João Botelho, Pedro Góis, Antonio Pascoal, Jorge Ribeiro, Miguel Ribeiro, Manuel Rufino, Luís Sebastião, and Henrique Silva. The MEDUSA class of autonomous marine vehicles and their role in EU projects. In *OCEANS 2016*, pages 1–10. IEEE, 2016.

[31] Marco Bibuli, Gabriele Bruzzone, Massimo Caccia, and Lionel Lapierre. Path-following algorithms and experiments for an unmanned surface vehicle. *Journal of Field Robotics*, 26(8), 2009.

[32] T. Oliveira, A. P. Aguiar, and P. Encarnação. Moving path following for unmanned aerial vehicles with applications to single and multiple target tracking problems. *IEEE Transactions on Robotics*, 32(5):1062–1078, 2016.

[33] M. F. Reis, R. P. Jain, A. P. Aguiar, and J. B. de Sousa. Robust moving path following control for robotic vehicles: Theory and experiments. *IEEE Robotics and Automation Letters*, 4(4):3192–3199, 2019.

[34] A Pedro Aguiar and João P Hespanha. Trajectory-tracking and path-following of underactuated autonomous vehicles with parametric modeling uncertainty. *IEEE Transactions on Automatic Control*, 52(8):1362–1379, 2007.

[35] Arthur GO Mutambara. *Decentralized Estimation and Control for Multisensor Systems*. CRC Press, 1998.

[36] K. Reif, S. Gunther, E. Yaz, and R. Unbehauen. Stochastic stability of the discrete-time extended Kalman filter. *IEEE Transactions on Automatic Control*, 44(4):714–728, April 1999.

[37] Reza Ghabcheloo, A Pedro Aguiar, Antnio Pascoal, Carlos Silvestre, Isaac Kaminer, and J Hespanha. Coordinated path-following in the presence of communication losses and time delays. *SIAM journal on control and optimization*, 48(1):234–265, 2009.
[38] Nguyen T. Hung, Antonio M. Pascoal, and Tor A. Johansen. Cooperative path following of constrained autonomous vehicles with model predictive control and event triggered communications. *International Journal of Robust and Nonlinear Control*, 2020.
[39] Francisco C. Rego, Nguyen T. Hung, Colin N. Jones, Antonio M. Pascoal, and A. Pedro Aguiar. Cooperative path-following control with logic-based communications: Theory and practice. Navigation and Control of Autonomous Marine Vehicles, chapter 8. IET, 2019.
[40] Wei Ren and Randal W Beard. *Distributed consensus in multi-vehicle cooperative control*. Springer, 2008.
[41] Eduardo D Sontag. Input to state stability: Basic concepts and results. In *Nonlinear and optimal control theory*, pages 163–220. Springer, 2008.
[42] Khalil Hassan. *Nonlinear systems*. Prentice Hall, New Jewsey, 3rd edition, 2002.

VIII. Appendix

A. Proof of Lemma 2

We first prove the result for the controller given by (24). Clearly, with (24), $e_\gamma(t) = 0$ for all t. Consider the Lyapunov function candidate $V_1 = \frac{1}{2}\|\mathbf{e}_\mathrm{p}\|^2$, yielding $\dot{V}_1 = \mathbf{e}_\mathrm{p}^\top \dot{\mathbf{e}}_\mathrm{p}$. Substituting (24) and (21) in $\dot{V}_1$, and noting that $\mathbf{e}_\mathrm{p}^\top S(\boldsymbol{\omega})\mathbf{e}_\mathrm{p} = 0$ for all $\mathbf{e}_\mathrm{p}$ and $\boldsymbol{\omega}$, we obtain $\dot{V}_1 = -\mathbf{e}_\mathrm{p}^\top K_\mathrm{p}\mathbf{e}_\mathrm{p} \leq -\lambda_2(K_\mathrm{p})\|\mathbf{e}_\mathrm{p}\|^2$ for all $\mathbf{e}_\mathrm{p}$. Thus, we conclude that $\mathbf{e}_\mathrm{p}$ converges to zero exponentially fast.

We now prove the theorem for the controller given by (25). Consider the Lyapunov function candidate KF

$$V_2(\mathbf{e}) = \|\mathbf{e}\|^2 = \frac{1}{2}\|\mathbf{e}_\mathrm{p}\|^2 + \frac{1}{2}e_\gamma^2. \tag{65}$$

Its time derivative is given by $\dot{V}_2 = \mathbf{e}_\mathrm{p}^\top \dot{\mathbf{e}}_\mathrm{p} + e_\gamma \dot{e}_\gamma$. Substituting (25) and (21) in $\dot{V}_2$ yields $\dot{V}_2 = -\mathbf{e}_\mathrm{p}^\top K_\mathrm{p}\mathbf{e}_\mathrm{p} - k_\gamma e_\gamma^2$. Let

$$K = \mathrm{diag}(K_\mathrm{p}, k_z). \tag{66}$$

Then, $\dot{V}_2 = -\mathbf{e}^\top K\mathbf{e} \leq -\lambda_{\min}(K)\|\mathbf{e}\|^2 < 0$ for all $\mathbf{e} \neq \mathbf{0}$. We conclude that the origin of $\mathbf{e}$ is GES. ■

B. Proof of Theorem 1

We only prove the theorem for the controller (29). The proof for the controller (28) is easier and can be done similarly. For the shake of clarity, let $\tilde{\mathbf{q}}$ and $\tilde{\boldsymbol{v}}$ be the target's position and velocity estimation errors, i.e. $\tilde{\mathbf{x}} = \mathrm{col}(\tilde{\mathbf{q}}, \tilde{\boldsymbol{v}})$. From (31), it follows that

$$\tilde{\mathbf{q}} = \hat{\mathbf{q}} - \mathbf{q}, \quad \tilde{\boldsymbol{v}} = \hat{\boldsymbol{v}} - \boldsymbol{v}. \tag{67}$$

From (19) and (27), we obtain

$$\hat{\mathbf{e}}_\mathrm{p} = \mathbf{e}_\mathrm{p} - R^\top(\boldsymbol{\eta})(\hat{\mathbf{q}} - \mathbf{q}) \overset{(67)}{=} \mathbf{e}_\mathrm{p} - R^\top(\boldsymbol{\eta})\tilde{\mathbf{q}}. \tag{68}$$

Further, substituting (29) in (21) and (23) yields

$$\begin{aligned} \dot{\mathbf{e}}_\mathrm{p} &= -S(\boldsymbol{\omega})\mathbf{e}_\mathrm{p} + R^\top(\boldsymbol{\eta})\left(\tilde{\boldsymbol{v}} - \mathbf{r}'(\gamma)e_\gamma\right) - K_\mathrm{p}\hat{\mathbf{e}}_\mathrm{p} \\ \dot{e}_\gamma &= -k_\gamma e_\gamma + \hat{\mathbf{e}}_\mathrm{p}^\top R^\top(\boldsymbol{\eta})\mathbf{r}'(\gamma). \end{aligned} \tag{69}$$

Consider again the Lyapunov function candidate V_2 given by (65). Taking the time derivative of V_2, and substituting (67)-(69) in $\dot{V}_2$, we obtain

$$\begin{aligned} \dot{V}_2 &= \mathbf{e}_\mathrm{p}^\top \dot{\mathbf{e}}_\mathrm{p} + e_\gamma \dot{e}_\gamma \\ &= -\mathbf{e}^\top K\mathbf{e} + \mathbf{e}_\mathrm{p}^\top R^\top(\boldsymbol{\eta})\tilde{\boldsymbol{v}} + \mathbf{e}_\mathrm{p}^\top K_\mathrm{p} R^\top(\boldsymbol{\eta})\tilde{\mathbf{q}} - e_\gamma \tilde{\mathbf{q}}^\top \mathbf{r}'(\gamma) \\ &= -\mathbf{e}^\top K\mathbf{e} + \mathbf{e}^\top \boldsymbol{\Phi} + \mathbf{e}_\mathrm{p}^\top K_\mathrm{p} R^\top(\boldsymbol{\eta})\tilde{\mathbf{q}}, \end{aligned} \tag{70}$$

where $\boldsymbol{\Phi} \triangleq \mathrm{col}\left(R^\top(\boldsymbol{\eta})\tilde{\boldsymbol{v}}, -\tilde{\mathbf{q}}^\top \mathbf{r}'(\gamma)\right)$. Furthermore,

$$\begin{aligned} \|\boldsymbol{\Phi}\|^2 &= \left\|R^\top(\boldsymbol{\eta})\tilde{\boldsymbol{v}}\right\|^2 + \left\|\tilde{\mathbf{q}}^\top \mathbf{r}'(\gamma)\right\|^2 \\ &\leq \|\tilde{\boldsymbol{v}}\|^2 + \|\mathbf{r}'(\gamma)\|^2\|\tilde{\mathbf{q}}\|^2 \\ &\leq \mu\|\tilde{\mathbf{x}}\|^2, \end{aligned} \tag{71}$$

where $\mu \triangleq \max_\gamma\{1, \|\mathbf{r}'(\gamma)\|^2\}$. Note that in (71) we used the fact that multiplying a vector on the left by a rotation matrix does not change the length of the vector. Furthermore, $\mathbf{e}_\mathrm{p}^\top K_\mathrm{p} R^\top(\boldsymbol{\eta})\tilde{\mathbf{q}} \leq \|\mathbf{e}\|\|K\|\|\tilde{\mathbf{x}}\|$. Substituting (71) in (70) yields

$$\begin{aligned} \dot{V}_2 &\leq -\lambda_{\min}(K)\|\mathbf{e}\|^2 + (\sqrt{\mu} + \|K\|)\|\mathbf{e}\|\|\tilde{\mathbf{x}}\| \\ &\leq -(1-\theta)\lambda_{\min}(K)\|\mathbf{e}\|^2, \quad \forall \|\mathbf{e}\| \geq (\sqrt{\mu} + \|K\|)\|\tilde{\mathbf{x}}\|/\theta \end{aligned} \tag{72}$$

with any $\theta \in (0, 1)$. Invoking Theorem 4.19 in [42], we conclude that the tracking error system is ISS respect to the state $\mathbf{e}$ and the input $\tilde{\mathbf{x}}$. This implies that there exist $\beta \in \mathcal{KL}$ and $\alpha \in \mathcal{K}$ functions such that (32) is satisfied. ■

C. Proof of Lemma 3

Consider a Lyapunov function candidate, defined as

$$V_\mathrm{c} = \boldsymbol{\xi}^\top R\boldsymbol{\xi}/2, \tag{73}$$

where $R \succ 0$ is a diagonal matrix defined in Lemma 1. The time derivative of the Lyapunov function is given by

$$\dot{V}_\mathrm{c} = \boldsymbol{\xi}^\top R\dot{\boldsymbol{\xi}} \overset{(58)}{=} -k_\mathrm{c}\boldsymbol{\xi}^\top RL\boldsymbol{\xi} + \boldsymbol{\xi}^\top RW\mathbf{e}_\gamma.$$

Because $\boldsymbol{\xi}$, defined in (55), is orthogonal to $\mathbf{1}$, using Definition 1, it follows that

$$\dot{V}_\mathrm{c} \leq -k_\mathrm{c} r_{\min}\|\boldsymbol{\xi}\|^2 + \|\boldsymbol{\xi}\|\|RW\|\|\mathbf{e}_\gamma\|, \tag{74}$$

where $r_{\min} := \min_{i=1}^N r_i$. Because $\|\mathbf{e}_\gamma\| \leq \|\mathbf{e}\|$, we obtain

$$\begin{aligned} \dot{V}_\mathrm{c} &\leq -k_\mathrm{c} r_{\min}\|\boldsymbol{\xi}\|^2 + \|RW\|\|\mathbf{e}\| \\ &\leq -(1-\theta)k_\mathrm{c} r_{\min}\|\boldsymbol{\xi}\|^2 \qquad \forall \|\boldsymbol{\xi}\| \geq \frac{\|RW\|}{\theta k_\mathrm{c} r_{\min}}\|\mathbf{e}\| \end{aligned} \tag{75}$$

with any $\theta \in (0, 1)$. Invoking Theorem 4.19 in [42], we conclude that the coordination error system is ISS respect to the state $\boldsymbol{\xi}$ and the input $\mathbf{e}$. ■

D. Proof of Lemma 4

We only prove the result for the controller (50). The proof for the controller (49) is easier and can be done similarly. To this end, consider the Lyapunov function candidate V_e, defined as

$$V_\mathrm{e}(\mathbf{e}) = \frac{1}{2}\sum_{i=1}^N \left\|\mathbf{e}^{[i]}\right\|^2 = \frac{1}{2}\sum_{i=1}^N \left\|\mathbf{e}_\mathrm{p}^{[i]}\right\|^2 + (e_\gamma^{[i]})^2 \tag{76}$$

Note that with this definition

$$V_\mathrm{e}(\mathbf{e}) = \sum_{i=1}^N V_2(\mathbf{e}^{[i]}),$$

where V_2 is given by (65). Using a computation similar to that in the proof of Theorem 1, we obtain

$$\dot{V}_2(\mathbf{e}^{[i]}) \leq -\lambda_{\min}(K)\left\|\mathbf{e}^{[i]}\right\|^2 + (\sqrt{\mu} + \|K\|)\left\|\mathbf{e}^{[i]}\right\|\left\|\tilde{\mathbf{x}}^{[i]}\right\| \tag{77}$$

which is inherited from (72). Therefore,

$$\begin{aligned}\dot{V}_{\rm e} &\leq \sum_{i=1}^{N} \dot{V}_2(\mathbf{e}^{[i]}) \leq -\lambda_{\min}(K)\|\mathbf{e}\|^2 + (\sqrt{\mu} + \|K\|)\|\mathbf{e}\|\|\tilde{\mathbf{x}}\|, \\ &\leq -\lambda_{\min}(K)(1-\theta)\|\mathbf{e}\|^2, \quad \forall \|\mathbf{e}\| \geq \frac{\sqrt{\mu} + \|K\|}{\theta\lambda_{\min}(K)}\|\tilde{\mathbf{x}}\| \end{aligned} \tag{78}$$

with $\mathbf{e} \triangleq [\mathbf{e}^{[1]}, ..., \mathbf{e}^{[N]}]^\top$ and $\tilde{\mathbf{x}} = [\tilde{\mathbf{x}}^{[1]}, ..., \tilde{\mathbf{x}}^{[N]}]^\top$ and $\theta \in (0, 1)$. Invoking Theorem 4.19 in [42], we conclude that the complete DEC system is ISS respect to the state $\mathbf{e}$ and the input $\tilde{\mathbf{x}}$. ■

E. Simulation parameters

TABLE I: Parameters for simulations in 2-D

	Parameters
Target's trajectory	$\mathbf{q} = [20\sin(0.01t + \pi), 0.3t]^\top$(m)
Range measurement	$\sigma = 0.5$m
S-T curve	$\bar{\omega} = 0.05$ rad/s $r_{\rm x}^{[i]} = r_{\rm y}^{[i]} = 30$m $\quad \forall i = 1, ..., 3$
Tracking Controller	$\boldsymbol{\epsilon} = [\text{-}0.5, 0]^\top$, $K_{\rm p} = \text{diag}([0.4, 0.2])$, $k_\gamma = 500$
Coordination Controller	$k_c = 0.2$
DEKF	$V^{[i]} = 10 \quad \forall i = 1, ..., 3$ $Q = 10^{-3}\text{diag}(1, 1, 0.1, 0.1)$ $\pi^i = \pi^j = 0.5 \quad \forall i = 1, ..., 3$ and $j \in \mathcal{N}_{\rm in}^{[i]}$ $T_{\rm s} = 2$s

TABLE II: Parameters for simulations in 3-D

	Parameters
Targets trajectory	$\mathbf{q} = [30\sin(0.01t + \pi), 0.1t, \text{-}0.5t]^\top$(m)
Range measurement	$\sigma = 0.5$m
S-T curve	$\bar{\omega} = 0.1$ rad/s $r_{\rm x}^{[i]} = r_{\rm y}^{[i]} = 80$m, $r_{\rm z}^{[i]} = 50$m $\quad \forall i = 1, ..., 3$
Tracking Controller	$\boldsymbol{\epsilon} = [\text{-}1, \text{-}1, 0]^\top$, $K_p = \text{diag}([0.2, 0.2, 0.2])$, $k_\gamma = 200$
Coordination Controller	$k_c = 0.2$
DEKF	$V^{[i]} = \sigma = 1 \quad \forall i = 1, ..., 3$ $Q = 10^{-3}\text{diag}(1, 1, 1, 0.1, 0.1, 0.1)$ $\pi^i = \pi^j = 0.5 \quad \forall i = 1, ..., 3$ and $j \in \mathcal{N}_{\rm in}^{[i]}$ $T_s = 2$s